

Greg Hancock
Associate Editor, Earth Surface Dynamics

January 18, 2021

Dear Dr. Greg Hancock,

Thank you for considering our manuscript 'Growing topography due to contrasting rock types in a tectonically dead landscape' for publication in ESurf. We are very grateful to the editor, the reviewer, and our colleagues for providing constructive feedback, allowing us to improve the manuscript.

We have edited the manuscript and the supplemental materials to address all issues raised during the review process. Please find our response letters in the following, where original comments are numbered and italicised, and our responses are coloured blue. We also provide an edited version of the article where specific changes made to the manuscript are highlighted. Line numbers in our response letters refer to this version of the manuscript with tracked changes.

The main changes we have made to the manuscript are: (i) we emphasised that our results agree with our knowledge on erosion processes in terrestrial landscapes; (ii) we emphasised that we are comparing how *catchment-averaged* denudation rates vary with changes in *mean* values of topographic relief, channel steepness and precipitation rates; (iii) we excluded our reference to 'persistence' (of denudation rates) as an explanation for relief growth; (iv) we defined 'equilibrium' more clearly; (v) we made several small revisions to clarify points or correct typos; and (vi) we included two figures to the Supplemental Materials.

We hope these modifications have significantly improved the manuscript and we thank the editor, the reviewer and the scientific community for the thoughtful suggestions.

Best regards,

Daniel Peifer

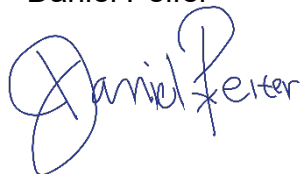


Table of Contents:

Response to RC1	3
Response to SC2	15
Response to SC4	19
Response to EC1	27
Response to SC1	31
Revised manuscript with tracked changes.....	32

Response to RC1: Interactive comment on "Growing topography due to contrasting rock types in a tectonically dead landscape" by Daniel Peifer et al.

Daniel Peifer et al.

peiferdaniel@gmail.com

Response to review

We thank the reviewer 1 for her/his thoughtful comments on our manuscript.

1. This is an innovative approach to a problem that has been around for a long time, and is worthy of publication. I have three substantive comments and a few minor ones.

We are pleased that the reviewer appreciates our work and perceives it as a valuable contribution.

2. The first substantive comment is that if the denudation rate data were stratified according to rock type it might then be that relief will be a correlate with denudation rate. After all I assume that the authors are not suggesting that the physics of erosion no longer applies, including the sine of slope function. To make the claim that you have contradicted established theory on the basis of this partial analysis is not supportable.

All else being equal, steeper slopes should lead to more rapid denudation rates. Our study area, however, is characterised by considerable spatial variations in lithology, where resistant and more erodible rock types are exposed in a slowly eroding, humid environment. Our results show that catchments underlain by what we infer to be resistant rocks, such as physically robust and chemically inert quartzites, are linked to higher catchment-averaged topographic metrics and lower catchment-averaged denudation rates than catchments in what we infer as more erodible rock types, such as gneisses and granitic rocks with abundant feldspars which are readily

weathered in such climate conditions. In this situation, we do not claim to have contradicted established theory. Instead, we show that substantial lateral variations in (inferred) rock strength in a post-orogenic setting obscure any regional relationships between catchment-averaged denudation rates and basin-wide topographic metrics and precipitation rates that might otherwise exist. Our contribution highlights that lateral and vertical variations in rock strength (in our case, inferred) are essential players in post-orogenic landscape dynamics, which have been overlooked to some degree despite widespread assertions that lithological resistance is of fundamental importance in landscape evolution. And we welcome the fact that such a viewpoint is now receiving more attention in modelling and empirical studies (e.g., Forte et al., 2016; Perne et al., 2017; Gallen, 2018; Bernard et al., 2019; Strong et al., 2019; Vasconcellos et al., 2019; Campforts et al., 2020; Gabet, 2020a, 2020b; Zondervan et al., 2020a, 2020b). Nevertheless, we removed our statement "appear to be contradictory to established theory, empirical studies and common sense", modifying the sentence to [lines 331-335]: *"The negative relationships we find between ¹⁰Be-derived catchment-averaged denudation rates and catchment-averaged values of topographic relief, channel steepness and precipitation rates, are counter-intuitive. However, such relationships are consistent with the stream-power model if one accounts for the magnitude of variations in the fluvial erosion efficiency coefficient (K) estimated for the study area."*

Following the reviewer suggestion, we have included a figure showing variations in catchment-averaged denudation rates with mean normalised channel steepness (extracted using a reference concavity of 0.45) for individual rock types (Fig. AR1). As expected, we observe that catchment-averaged denudation rates and mean normalised channel steepness may increase together for several rock types, though with such small sample sizes no such relationships are

statistically significant at the $\alpha = 0.05$ level except for catchments in phyllites. We conjecture that we did not find statistically significant positive relationships between these variables for every rock type because: (i) the relatively low range in values of topographic metrics for catchments underlain by the same rock types (for example, every catchment in gneisses and granite gneiss is characterised by low values of catchment-averaged normalised channel steepness); and (ii) internal variability in the fluvial erosion efficiency coefficient within each rock type (as discussed in the manuscript). Moreover, we note that the fluvial erosion efficiency coefficient incorporates controls other than rock type, which likely increases the internal variability in fluvial erosion efficiency in areas underlain by the same rock type. Nevertheless, we emphasise that we would expect denudation to increase together with topographic metrics in areas with the same fluvial erosion efficiency coefficient.

We have added Figure AR1 to the Supplemental Materials (as Fig. S5), referencing it in the Results section through an additional sentence [lines 264-266]: *"However, we observe that catchment-averaged denudation rates may increase together with mean values of topographic metrics and precipitation rates for individual rock types, although with such small sample sizes no such relationships are statistically significant at the $\alpha = 0.05$ level except for catchments in phyllites (Fig. 4, S6)."*

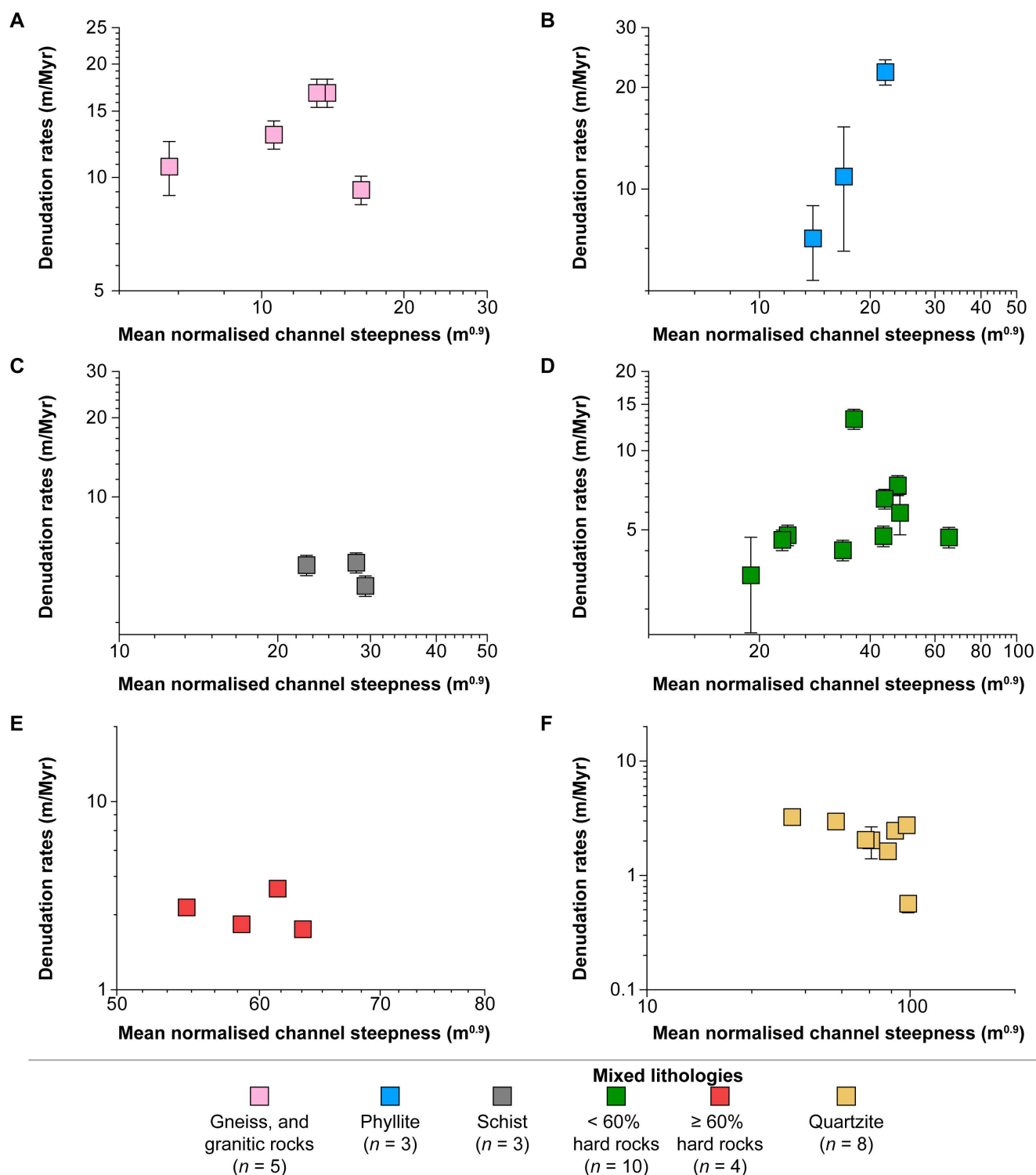


Figure AR1: Variations in catchment-averaged denudation rates with mean normalised channel steepness for individual rock types. Y-error bars show measurement uncertainties in the nuclide concentration as well as uncertainties related to the scaling method. Mixed lithology refers to catchments where a single lithology does not account for $\geq 75\%$ of the catchment area.

3. The second is that the term 'equilibrium', 'steady state', and 'quasi-equilibrium' are used at many places without definition or explanation. This is a concern as, I am sure the authors know, the concept of equilibrium in geomorphology is, to say the least, vexed. What do you mean by these terms and how do you justify your usage?

We agree with the reviewer that concepts such as 'equilibrium' and 'steady state' are best used when clearly defined. In this contribution, we refer to 'equilibrium' and 'steady state' implying a 'topographic equilibrium' in which topographic forms are constant through time and denudation rates are spatially invariant irrespective of differences in rock type or topographic relief; in this situation, rock uplift is balanced by erosion, and topographic relief is adjusted to rock strength so that everywhere is downwasting at the same rate (Hack, 1960; Montgomery, 2001). The 'topographic equilibrium' concept is somewhat problematic for post-orogenic landscapes given that rock uplift is necessary to maintain equilibrium (e.g., Kooi and Beaumont, 1996), yet some post-orogenic settings have been interpreted as in a topographic steady state, perhaps driven by isostatic denudational rebound (e.g. Matmon et al., 2003; Mandal et al., 2015). We rephrased our description of these concepts and interpretations to [lines 68-72]: *"These observations were interpreted, in several cases, as equilibrium adjustments where spatial variations in rock strength are balanced by variations in topographic relief so that everywhere is eroding at the same rate, with the corollary that topographic forms are constant through time in a 'topographic equilibrium' likely driven by isostatic uplift (e.g., Hack, 1960; Matmon et al., 2003; Scharf et al., 2013; Mandal et al., 2015)." To ensure consistency in using these concepts, we have excluded the term 'quasi-equilibrium' from the manuscript [line 313].*

4. The third substantive issue concerns denudation rate vs. averaging time. With one exception the denudation rates have averaging times less than 0.35Ma and there are a lot much less than

0.35Ma. It is necessary in my view to stratify the denudation rate data according to various averaging times to see if you get different results. You are asking a lot of an analysis that uses such a range of averaging times (27ka to 1.1Ma). And either exclude the rate at about 1.1Ma or explain it. I have added a graph of these data.

This remark is correct, and we did present one denudation rate estimate (sample ID: S5) with an average timescale much higher than the averaging timescale of all other denudation rate estimates. However, we do not consider such denudation rate estimate to be problematic for the conclusions of our study. First, measurements and averaging times (i.e., time taken for sand grains to be exhumed through the CRN production zone near the surface) are implicitly coupled and thus it is not possible to separate them; the slower the denudation rate, the longer the time averaged over. The "anomalous" denudation rate estimate (0.6 ± 0.1 m/Myr) was derived for a catchment in quartzite; all other estimates derived for catchments in quartzites yielded similarly low rates of denudation (ranging from 1.6 ± 0.2 to 3.3 ± 0.3 m/Myr). Thus, there is no indication that such a denudation rate estimate is somehow incorrect. Second, when we remove the "anomalous" denudation rate estimate from our analysis, we find that all of the relationships previously found between catchment-averaged denudation rates and mean topographic metrics and precipitation rates hold (see Fig. AR2). That being said, our sentence "Persistence of these denudation rates (averaged over timescales up to 1.1 Myr; Table S1)" [line 367-368] is misleading, and we removed it from the manuscript. We modified the manuscript to [lines 365-368]: *"Our findings indicate that high-relief uplands underlain by resistant bedrock are denuding more slowly than lower-relief surrounding areas associated with more erodible lithologies, with the corollary that topographic relief must still be growing instead of decaying in this tectonically quiescent landscape"*.

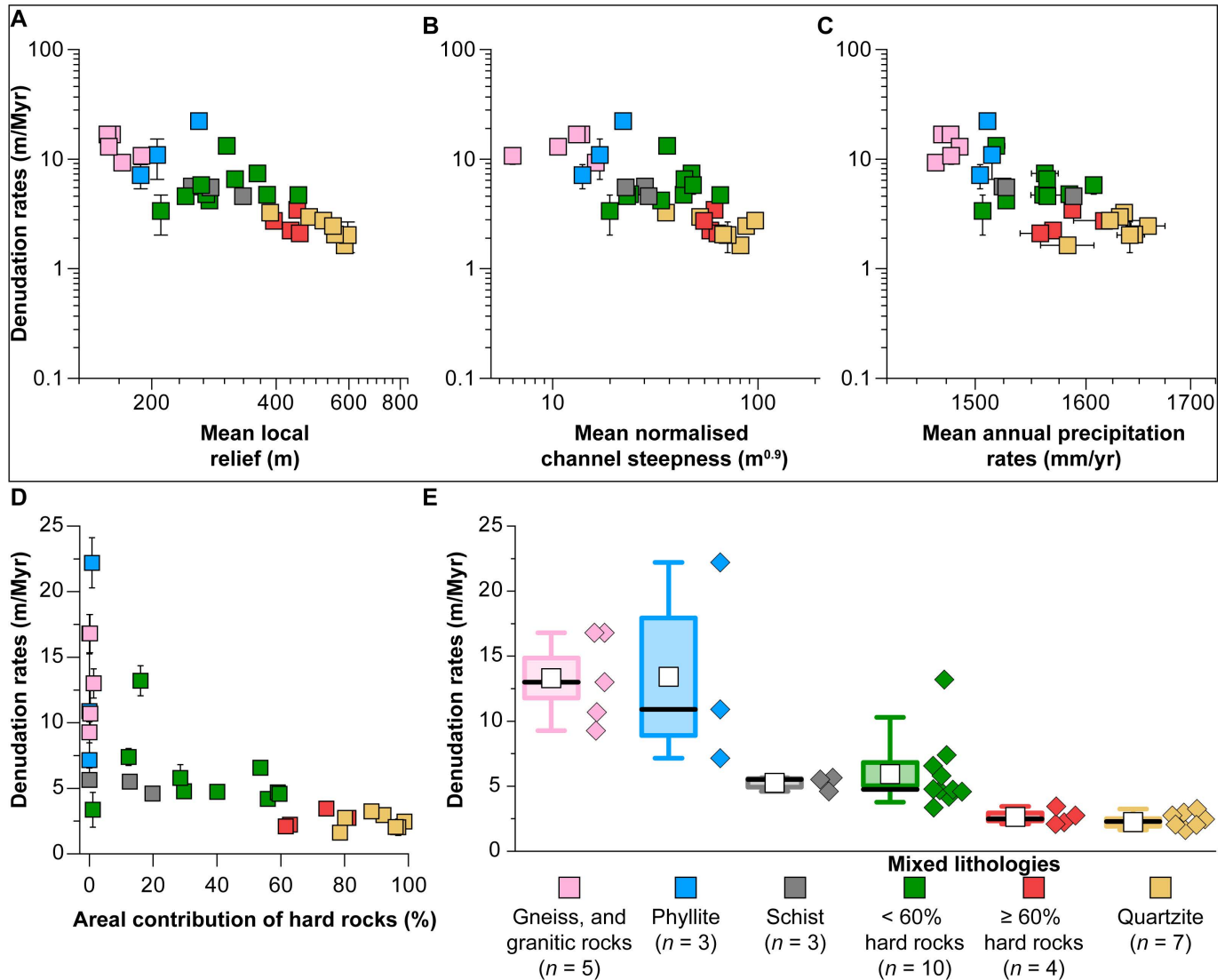


Figure AR2: Links between denudation rates, geomorphic parameters, and rock type in the study area excluding sample S5. Variations in catchment-averaged denudation rates with (A) mean local relief, (B) mean normalised channel steepness, (C) mean annual precipitation rates, and (D) percentage areal contribution of resistant rocks. Y-error bars show measurement uncertainties in the nuclide concentration as well as uncertainties related to the scaling method, and X-error bars indicate the SE of the mean. (E) Variations in catchment-averaged denudation rates per rock type, with the box on the left and raw data (diamonds) on the right. Box range represents the SE of the mean, whiskers show the interval between the 10th and 90th percentiles of the data, white squares show mean values, and thick black lines exhibit median values. Mixed lithology refers to catchments where a single lithology does not account for $\geq 75\%$ of the catchment area.

Minor comments

5. Line 39. Is it still called the Lachlan Fold Belt?

It is still referred to as Lachlan Fold Belt to the best of our knowledge. However, we modified the manuscript to [lines 38-40]: "Examples of ancient mountain belts marked by high elevations and

steep slopes include the Appalachian Mountains, several mountain ranges SE Brazil, the Cape Mountains, parts of the East Australian Highlands, the Ural Mountains, the Caledonides, the Western Ghats, and the Sri Lanka orogen (Fig. 1)."

6. Line 76. *What is semitropical? It is either tropical or it is not.*

We agree with the reviewer. We refer in the revised manuscript as "humid subtropical" [lines 14, 80, 119, 198, 272, 397] given that climate over the study area ranges from Cwa to Cwb in Köppen-Geiger's classification (Alvares et al., 2013). We modified the manuscript to include this information [lines 94-95], and we included Alvares et al. (2013) in our references.

7. Lines 96-101. *I would like to see a little more information about the accuracy of these estimates and whether or not this is a craton. It is called an ancient orogen at line 143.*

Thank you for this remark.

i) We modified the manuscript to describe the available data more thoroughly as [lines 102-111]:
"An array of geochronological data imply that the current topography is long-lived. These data include: a relatively large set of (U-Th)/He data ($n = 291$) and cosmogenic ^3He concentrations ($n = 71$) in iron oxides showing mineral precipitation ages as old as 55 Ma (varying from 55.3 ± 5.5 to 0.4 ± 0.1 Ma), and exposure ages ranging from 10.9 ± 1.2 to 0.2 ± 0.1 Ma, with age versus elevation relationships suggesting older ages and a more extended history of exposure in iron duricrust-covered plateaus at higher elevations (Monteiro et al., 2014, 2018); $^{40}\text{Ar}/^{39}\text{Ar}$ dating of Mn oxide grains collected in nine weathering profiles in the QF ($n = 174$ grains that produced reliable results) yielding ages ranging from 94.6 ± 5.5 to 12.3 ± 0.5 Ma, yet predominantly distributed between 30-60 Ma (Spier et al., 2006; Vasconcelos and Carmo, 2018); and low denudation rates (<3 m/Myr) implied by cosmogenic ^3He and ^{10}Be inventories (Monteiro et al.,

2018; Salgado et al., 2008)." We have added Monteiro et al. (2014) and Spier et al. (2006) to our references.

ii) The study area is a post-orogenic landscape with a polyphase deformation history, the last episode of which was ~500-450 Myr ago, and thus it is not a craton (see lines 97-99). We have not made any modifications to the manuscript based on this point as we feel that it is already set out clearly in the manuscript.

8. Line 342 *You cannot claim that the denudation rate has persisted from 1.1Ma on the basis of the existing analysis (see substantive comment three above). The 1.1Ma value may be an anomaly.*

Agreed. We removed such reference from the manuscript [lines 367-370] (see response 4).

9. Line 343. *Can you make this claim about flexural-isostatic compensation without modelling of this landscape? Or are you making an argument from theory. If the latter please make this clear.*

We are making this argument from theory. We modified the manuscript to [lines 365-374]: *"Our findings indicate that high-relief uplands underlain by resistant bedrock are denuding more slowly than lower-relief surrounding areas associated with more erodible lithologies, with the corollary that topographic relief must still be growing instead of decaying in this tectonically quiescent landscape. Furthermore, the expected isostatic compensation to denudational unloading (e.g., Bishop and Brown, 1992), which is a process that occurs at a much longer wavelength than the local changes in lithology and denudation rates (Gilchrist and Summerfield, 1990; Watts et al. 2000), implies that uplands and surrounding areas are equally isostatically uplifted in response to the regional denudation, likely resulting in a net reduction of mean*

elevation over time, but a slight increase in the heights of mountain peaks, as has been proposed by Molnar and England (1990)." We have also added Watts et al. (2000) to our references.

References

- Alvares, C.A., Stape, J.L., Sentelhas, P.C., de Moraes Gonçalves, J.L. and Sparovek, G.: Köppen's climate classification map for Brazil, Meteorol. Z., 22, 711–728, <https://doi.org/10.1127/0941-2948/2013/0507>, 2013.
- Bernard, T., Sinclair, H.D., Gailleton, B., Mudd, S.M. and Ford, M.: Lithological control on the post-orogenic topography and erosion history of the Pyrenees, Earth Planet. Sc. Lett., 518, 53–66, <https://doi.org/10.1016/j.epsl.2019.04.034>, 2019.
- Campforts, B., Vanacker, V., Herman, F., Vanmaercke, M., Schwanghart, W., Tenorio, G.E., Willems, P. and Govers, G.: Parameterisation of river incision models requires accounting for environmental heterogeneity: insights from the tropical Andes, Earth Surf. Dynam., 8, 447–447, <https://doi.org/10.5194/esurf-8-447-2020>, 2020.
- Forte, A.M., Yanites, B.J. and Whipple, K.X.: Complexities of landscape evolution during incision through layered stratigraphy with contrasts in rock strength, Earth Surf. Proc. Land., 41, 1736–1757, <https://doi.org/10.1002/esp.3947>, 2016.
- Gabet, E.J.: Lithological and structural controls on river profiles and networks in the northern Sierra Nevada (California, USA), GSA Bulletin, 132, 655–667, <https://doi.org/10.1130/B35128.1>, 2020a.
- Gabet, E.J.: River profile evolution by plucking in lithologically heterogeneous landscapes: Uniform uplift vs. tilting, Earth Surf. Proc. Land., 45, 1579–1588, [10.1002/esp.4832](https://doi.org/10.1002/esp.4832), 2020b.
- Gallen, S.F.: Lithologic controls on landscape dynamics and aquatic species evolution in post-orogenic mountains, Earth Planet. Sc. Lett., 493, 150–160, <https://doi.org/10.1016/j.epsl.2018.04.029>, 2018.
- Gilchrist, A.R. and Summerfield, M.A.: Differential denudation and flexural isostasy in formation of rifted-margin upwarps, Nature, 346, 739–742, <https://doi.org/10.1038/346739a0>, 1990.
- Hack, J.T.: Interpretation of erosional topography in humid temperate regions, Am. J. Sci., 258, 80–97, 1960.
- Kooi, H. and Beaumont, C.: Large-scale geomorphology: Classical concepts reconciled and integrated with contemporary ideas via a surface processes model. J. Geophys. Res.-Sol. Ea., 101, 3361–3386, <https://doi.org/10.1029/95JB01861>, 1996.

Mandal, S.K., Lupker, M., Burg, J.P., Valla, P.G., Haghypour, N. and Christl, M.: Spatial variability of ^{10}Be -derived erosion rates across the southern Peninsular Indian escarpment: A key to landscape evolution across passive margins, *Earth Planet. Sc. Lett.*, 425, 154–167, <https://doi.org/10.1016/j.epsl.2015.05.050>, 2015.

Matmon, A., Bierman, P.R., Larsen, J., Southworth, S., Pavich, M. and Caffee, M.: Temporally and spatially uniform rates of erosion in the southern Appalachian Great Smoky Mountains, *Geology*, 31, 155–158, [https://doi.org/10.1130/0091-7613\(2003\)031<0155:TASURO>2.0.CO;2](https://doi.org/10.1130/0091-7613(2003)031<0155:TASURO>2.0.CO;2), 2003.

Molnar, P. and England, P.: Late Cenozoic uplift of mountain ranges and global climate change: chicken or egg?, *Nature*, 346, 29–34, <https://doi.org/10.1038/346029a0>, 1990.

Monteiro, H.S., Vasconcelos, P.M., Farley, K.A., Spier, C.A. and Mello, C.L.: (U–Th)/He geochronology of goethite and the origin and evolution of cangas, *Geochim. Cosmochim. Ac.*, 131, 267–289, <https://doi.org/10.1016/j.gca.2014.01.036>, 2014.

Monteiro, H.S., Vasconcelos, P.M. and Farley, K.A.: A combined (U–Th)/He and cosmogenic ^3He record of landscape armoring by biogeochemical iron cycling, *J. Geophys. Res.-Earth*, 123, 298–323, <https://doi.org/10.1002/2017JF004282>, 2018.

Montgomery, D.R.: Slope distributions, threshold hillslopes, and steady-state topography, *Am. J. Sci.*, 301, 432–454, <https://doi.org/10.2475/ajs.301.4-5.432>, 2001.

Perne, M., Covington, M.D., Thaler, E.A. and Myre, J.M.: Steady state, erosional continuity, and the topography of landscapes developed in layered rocks, *Earth Surf. Dynam.*, 5, 85–100, <https://doi.org/10.5194/esurf-5-85-2017>, 2017.

Spier, C.A., Vasconcelos, P.M. and Oliviera, S.M.: $^{40}\text{Ar}/^{39}\text{Ar}$ geochronological constraints on the evolution of lateritic iron deposits in the Quadrilátero Ferrífero, Minas Gerais, Brazil, *Chem. Geol.*, 234, 79–104, <https://doi.org/10.1016/j.chemgeo.2006.04.006>, 2006.

Strong, C.M., Attal, M., Mudd, S.M. and Sinclair, H.D.: Lithological control on the geomorphic evolution of the Shillong Plateau in Northeast India, *Geomorphology*, 330, 133–150, <https://doi.org/10.1016/j.geomorph.2019.01.016>, 2019.

Vasconcelos, P.M. and Carmo, I.D.O.: Calibrating denudation chronology through $^{40}\text{Ar}/^{39}\text{Ar}$ weathering geochronology, *Earth-Sci. Rev.*, 179, 411–435, <https://doi.org/10.1016/j.earscirev.2018.01.003>, 2018.

Vasconcelos, P.M., Farley, K.A., Stone, J., Piacentini, T. and Fifield, L.K.: Stranded landscapes in the humid tropics: Earth's oldest land surfaces, *Earth Planet. Sc. Lett.*, 519, 152–164, <https://doi.org/10.1016/j.epsl.2019.04.014>, 2019.

Watts, A.B., McKerrow, W.S. and Fielding, E.: Lithospheric flexure, uplift, and landscape evolution in south-central England, *J. Geol. Soc.*, 157, 1169-1177, <https://doi.org/10.1144/jgs.157.6.1169>, 2000.

Willett, S.D. and Brandon, M.T.: On steady states in mountain belts, *Geology*, 30, 175–178, [https://doi.org/10.1130/0091-7613\(2002\)030<0175:OSSIMB>2.0.CO;2](https://doi.org/10.1130/0091-7613(2002)030<0175:OSSIMB>2.0.CO;2), 2002.

Zondervan, J.R., Stokes, M., Boulton, S.J., Telfer, M.W. and Mather, A.E.: Rock strength and structural controls on fluvial erodibility: Implications for drainage divide mobility in a collisional mountain belt. *Earth Planet. Sc. Lett.*, 538, 1–13, <https://doi.org/10.1016/j.epsl.2020.116221>, 2020a.

Zondervan, J.R., Whittaker, A.C., Bell, R.E., Watkins, S.E., Brooke, S.A. and Hann, M.G: New constraints on bedrock erodibility and landscape response times upstream of an active fault, *Geomorphology*, 351, 1–14, <https://doi.org/10.1016/j.geomorph.2019.106937>, 2020b.

Response to SC2: Interactive comment on "Growing topography due to contrasting rock types in a tectonically dead landscape" by Daniel Peifer et al.

Daniel Peifer et al.

peiferdaniel@gmail.com

Response to SC2

1. The preprint presents some great field, laboratory, and computational work, interprets the results in a reasonable way and provides insightful conclusions. While my current opinion of it is excellent, the first impression was not. It took me a lot of re-reading to figure out that it makes sense. Let me explain in order to help make the final article more attractive for casual readers as well. The claim in line 240 "denudation rates are negatively correlated with normalised channel steepness" is surprising when one looks at Equation (5b) which implies that fluvial erosion and steepness are positively correlated. Is denudation negatively correlated with fluvial erosion? Is there a mistake? Steepness is not a quantity that can be measured in nature, it is derived and requires a choice of concavity. Could a poor choice lead to this unexpected result? In fact, everything is fine. The context and Figure 4B tell that catchment-averaged normalised channel steepness is being discussed. Figures 4E (the link between denudation rate and rock type) and 5C (the link between the catchment-averaged local relief and rock type) provide results that come directly from measurements and are easier to interpret:

- hard rocks denude more slowly;*
- as a consequence, relief on them is higher.*

Channel steepness on hard rocks is thus higher as well (for a reasonable concavity). Therefore, there is a negative correlation between the steepness and the denudation rate when speaking

of catchment averages. Assuming I'm a typical reader, a typical reader would understand this point with less effort if the results from figures 4E and 5C (which directly describe nature and are in agreement with one's expectations) were mentioned first and emphasised more.

Dear Matija Perne,

Thank you for such thoughtful and helpful comments; it is rewarding to receive your feedback that our manuscript is a valuable contribution. We are very grateful that you read our manuscript so carefully and took the time to write such constructive inputs.

We took your comments on board when revising the manuscript. First, we modified the manuscript in several places [lines 15, 255, 258, 261, and 263] to emphasise that we are comparing how catchment-averaged denudation rates vary with changes in mean values of local relief, normalised channel steepness and mean annual precipitation.

Second, we have added a sentence at the end of the first paragraph of the 'results' section to emphasise that our results indeed agree with our knowledge on erosion processes in terrestrial landscapes [lines 264-266]: *"However, we observe that catchment-averaged denudation rates may increase together with mean values of topographic metrics and precipitation rates for individual rock types, although with such small sample sizes no such relationships are statistically significant at the $\alpha = 0.05$ level except for catchments in phyllites (Fig. 4, S6)."* We have also added Figure AR1 to the Supplemental Materials (see response 2 to RC1).

3. I believe the units for K depend on the exponent m (see equation 4) and are not fixed for a given concavity. In this case, the claim in line 219 that the unit follows from the reference concavity is not exactly right. The results referred to around the line 272 with $n = 2$ may be given with a wrong unit, assuming the reference concavity was the same. Conversely, different

concavity indices could result in the same unit for K , so not every K with the same unit has the same meaning (in contrast with what line 317 implies). All of it has no consequence for the conclusions of the article.

The critical point Matija is concerned in his comment of units for K is that we cannot directly compare K values for $n = 1$ and $n = 2$ for our fixed, topographically-informed concavity (concavity = 0.45), because the units change. This remark is correct, and we should be more cautious in how we report these results.

We modified the sentences addressing this comparison to: i) [lines 234-235] "*We extracted k_{sn} using 0.45 as the reference concavity which, assuming $m = 0.45$ and $n = 1$, yields K values with units of $m^{0.1}/\text{yr}$.*"; and ii) [lines 293-295] "*When the slope exponent n is equal to 2, we find absolute values of K to be more than one order of magnitude lower for every catchment (assuming $m = 0.9$ and $n = 2$, derived values of K have units of $m^{-0.8}/\text{yr}$).*" We have also modified Fig. 6, so it shows the correct units. Nevertheless, the statement we make from the comparison is the most important, that changing n does not change the relationships we find between catchment lithology, catchment-averaged denudation rates, and the fluvial erosion efficiency coefficient.

Although we agree with Matija's statement that "different concavity indices could result in the same unit for K , so not every K with the same unit has the same meaning", for a given m (for instance, 0.4), not every choice of n result in reasonable values of concavity. For example, assuming $m = 0.4$ (and the units for K depend on this exponent m), for $n = 1$ (concavity = 0.4, which is a reasonable value); whereas for $n = 2$ (concavity = 0.2); $n = 3$ (concavity = 0.1333333333333333); and $n = 4$ (concavity = 0.1). Thus, we have not changed our statement [lines 342-344]: "*To compare our constraints on the fluvial erosion efficiency coefficient with*

published estimates of K , we also calculate K in units of $m^{0.2}/yr$, as reported in several studies (e.g., Stock and Montgomery, 1999; Whipple et al., 2000b; Kirby and Whipple, 2001)."

4. There are also a few little things I'd like to mention. The terms 'steepness' and 'steepness index' seem to mean the same thing, similarly for 'concavity' and 'concavity index'. Consistent use of one version would eliminate any doubt.

Agreed. We have now a consistent use of 'channel steepness' and 'channel concavity' in the manuscript.

5. The DOI of Perne et al., 2017 appears to be wrong.

Thanks for this remark. We made sure every DOI is correct in the revised manuscript.

6. In the caption of the Figure S2, the description of subplots (A, C, E) should refer to (A, B, C).

Fixed.

7. Regarding the lines 341 and 342, referring to persistence seems unnecessary for the relief to be growing (relief growth is not associated with a particular timescale so no particular averaging period is necessary). The persistence implies that relief has on average been growing throughout the averaging time scale.

Agreed. We excluded our reference to 'persistence', modifying our sentence to [lines 365-368]:
"Our findings indicate that high-relief uplands underlain by resistant bedrock are denuding more slowly than lower-relief surrounding areas associated with more erodible lithologies, with the corollary that topographic relief must still be growing instead of decaying in this tectonically quiescent landscape".

Response to SC4: Interactive comment on "Growing topography due to contrasting rock types in a tectonically dead landscape" by Daniel Peifer et al.

Daniel Peifer et al.

peiferdaniel@gmail.com

Response to SC4

1. Two points:

Your study is exhumation of a passive margin landscape. There's some good work by Zondervan et al 2020 Earth and Planetary Science Letters who look at rock strength / erodibility in a collisional mountain belt (High Atlas, Morocco), but in a post orogenic phase (i.e. tectonically dead / quiescent). The relevance of this Zondervan work is that it is an inverted rift, with a post-rift, syn-rift cover and basement craton geology and thus the patterns and directions of exhumation are all rock strength and structure controlled.

Dear Martin Stokes,

Thank you very much for your constructive comments.

We agree that Zondervan et al. (2020) is relevant to our manuscript, particularly as it demonstrates (using robust methods that are important to our manuscript) that variations in rock strength (and its influence in the fluvial erodibility) play a fundamental role in the dynamics and evolution of a collisional mountain belt in a post-orogenic phase. Therefore, we have added Zondervan et al. (2020) to our references.

2. The Brazilian passive margin is considered to be reactivated tectonically within the Neogene, as per the very large volume of local Brazilian case study geomorphology / structural literature, which I think warrants some explanation.

Our study area, the Quadrilátero Ferrífero (QF), is not a passive margin. The QF lies in the southeastern edge of the São Francisco Craton (SFC; Fig. AR3), far away from the coastline (~350 km in a straight line from the Atlantic Ocean; see Fig. 2), in the boundary between the SFC and the Mantiqueira Province. The SFC consists of an Archean-Paleoproterozoic block that has not experienced major tectonic and magmatic events since ~1900 Ma (Almeida et al., 1981; Alkmim and Martins-Neto, 2012; Aguilar et al., 2017) encircled (on all sides) by Neoproterozoic- to Early Ordovician Brasiliano orogenic belts that developed during the Brasiliano/Pan-African collage of West Gondwana (Endo and Fonseca, 1992; Alkmim and Teixeira, 2017; Heilbron et al., 2017).

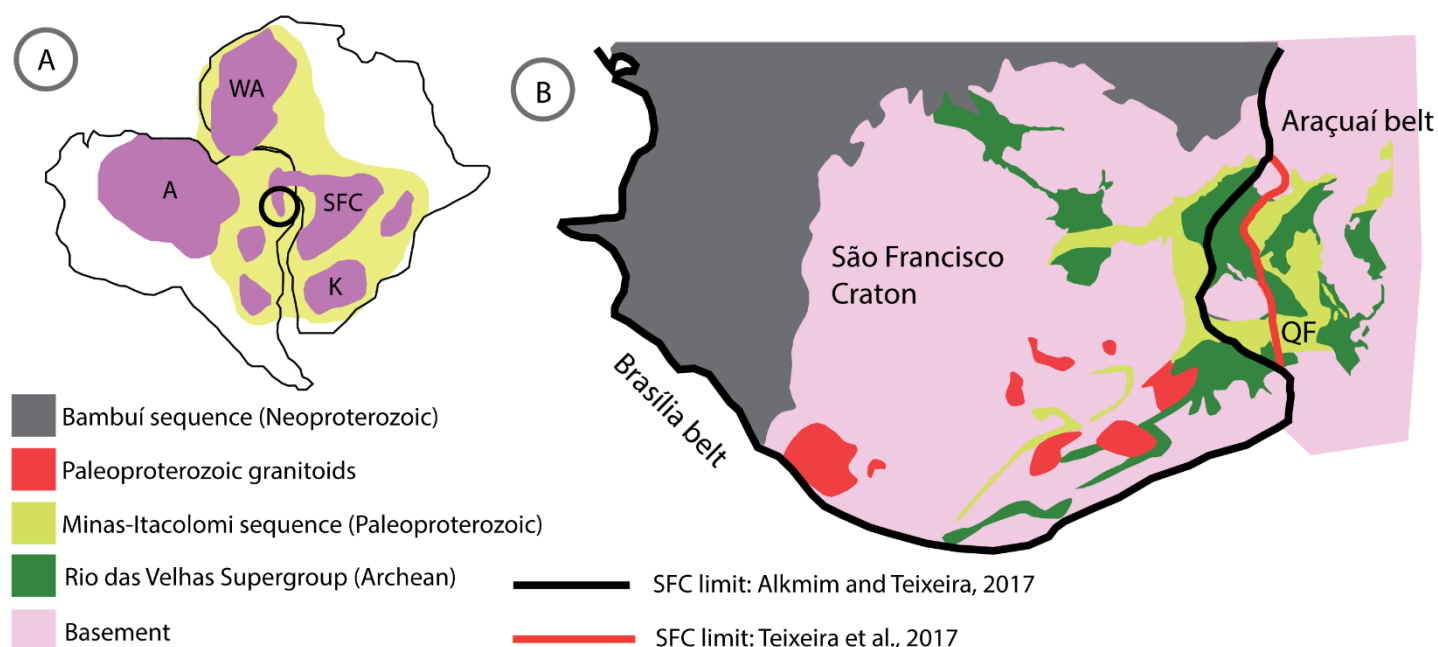


Figure AR3: Simplified geology of the QF. (A) The tectonic context of the assembly of West Gondwana by the end of the Proterozoic: cratons (in purple) surrounded by Neoproterozoic mobile belts (in yellow); in this reconstruction, the São Francisco Craton includes the Congo Craton, now in Africa. Note that there is some controversy about the position of the SFC's limit. Cratons: A – Amazonian; WA – West Africa; SFC – São Francisco-Congo; K – Kalahari. Modified from Alkmim and Martins-Neto (2012).

The QF experienced a polyphase deformation history resulting in a complex structural framework which is generally considered to be the result of three different kinematic phases identified using cross-cutting relationships and kinematic criteria (e.g., Chemale Jr et al., 1994;

Alkmim and Marshak, 1998) yet with limited absolute age constraints (Farina et al., 2016; Alkmim and Teixeira, 2017). In summary, the oldest phase is a Rhyacian collision related to a set of NE-SW-trending, NW-verging regional-scale folds (Alkmim and Marshak, 1998; Farina et al., 2016; Alkmim and Teixeira, 2017). The second phase is related to an extensional event associated with the formation of a dome-and-keel geological architecture, comprising basement domes and surrounding supracrustal synclines, likely in a context of the extensional collapse of the Rhyacian orogen (Chemale Jr et al., 1994; Alkmim and Marshak, 1998). The youngest phase is a Neoproterozoic- to Early Ordovician Brasiliano (650-480 Ma) compressional event, related to the amalgamation of West Gondwana, with the development of a west-verging thrust system that overprinted and reactivated pre-existing structures (Chemale Jr et al., 1994; Alkmim and Marshak, 1998; Alkmim and Teixeira, 2017). This compressional event affected mainly the eastern part of the QF, with the intensity of deformation decreasing westward; a series of WNW-verging faults and thrust cuts the entire Precambrian section of the eastern part of the QF (Chemale Jr et al., 1994; Alkmim and Marshak, 1998; Alkmim and Teixeira, 2017).

There is, indeed, a robust body of observational constraints, including thermochronological, sedimentary and geomorphic data, indicating a complex post-rift tectonic reactivation scenario in the elevated passive margin of SE Brazil, yet the available data suggest a much more stable tectonic history in the continental interior (e.g., Gallagher et al., 1994; Carmo, 2005; Tello Saenz et al., 2005; Hiruma et al., 2010; Cogné et al., 2011, 2012; Jelinek et al., 2014; Engelman de Oliveira et al., 2016; Krob et al., 2019; van Ranst et al., 2020; Fonseca et al., 2020). In this situation, the QF is not part of the elevated passive margin of SE Brazil, being located, instead, more in the deep interior of the continent (see Fig. 2), and there is no evidence that the QF was

directly affected by the continental breakup. Furthermore, the geochronological data available indicate that the study area's topography is long-lived (see lines 102-111).

Nonetheless, some authors did hypothesise that some areas in the QF, mainly the eastern half of the study area, experienced Cenozoic deformation based on field evidence of post-deformation in small and spatially restricted Cenozoic deposits (e.g., Saadi, 1992; Sant'anna et al., 1997; see lines 111-113); see the attached Fig. AR4 for the (limited) spatial distribution of Cenozoic units in the QF. Our sampling design included catchments spanning the range of topographic relief and bedrock lithologies in the study area, yet much of our data is derived from catchments located in the easternmost part of the QF (i.e., catchments P4, P5, P6, P7, P8, P12, P13, S5, S6 and S7; see Fig. 3). These catchments cover the area with the most pronounced topographic relief in the QF (Fig. 2), which is also characterised by the presence of many old structural anisotropies resulting from intense deformation experienced by this region during the Neoproterozoic- to Early Ordovician Brasiliano compressional event (Chemale Jr et al., 1994; Alkmim and Marshak, 1998; Alkmim and Teixeira, 2017). Our results show that these catchments in quartzites (i.e., catchments P7, P8, P12, P13, S5, S6 and S7) denude at low rates irrespective of their high topographic relief, with a minimum denudation rate of 0.6 ± 0.1 m/Myr for the catchment with the most pronounced topography (see Table S1). We did not observe any evidence of the influence of ongoing tectonic activity in our ^{10}Be -derived catchment-averaged denudation rates.

We modified the first sentence of the 'geologic setting' section to [lines 86-87]: "*The study area is the Quadrilátero Ferrífero (Brazil), one of Brazil's highest elevation areas, with a peak elevation of 2,076 m, located in the continental interior ~350 km away in a straight line from the Atlantic Ocean (Fig. 2).*" We have also added Fig. AR4 to the Supplemental Materials (as Fig.

S1) [see lines 111-114]. However, we have not made any other modifications to the manuscript based on these statements as we feel that the context and implications of our results are already set out clearly in the manuscript.

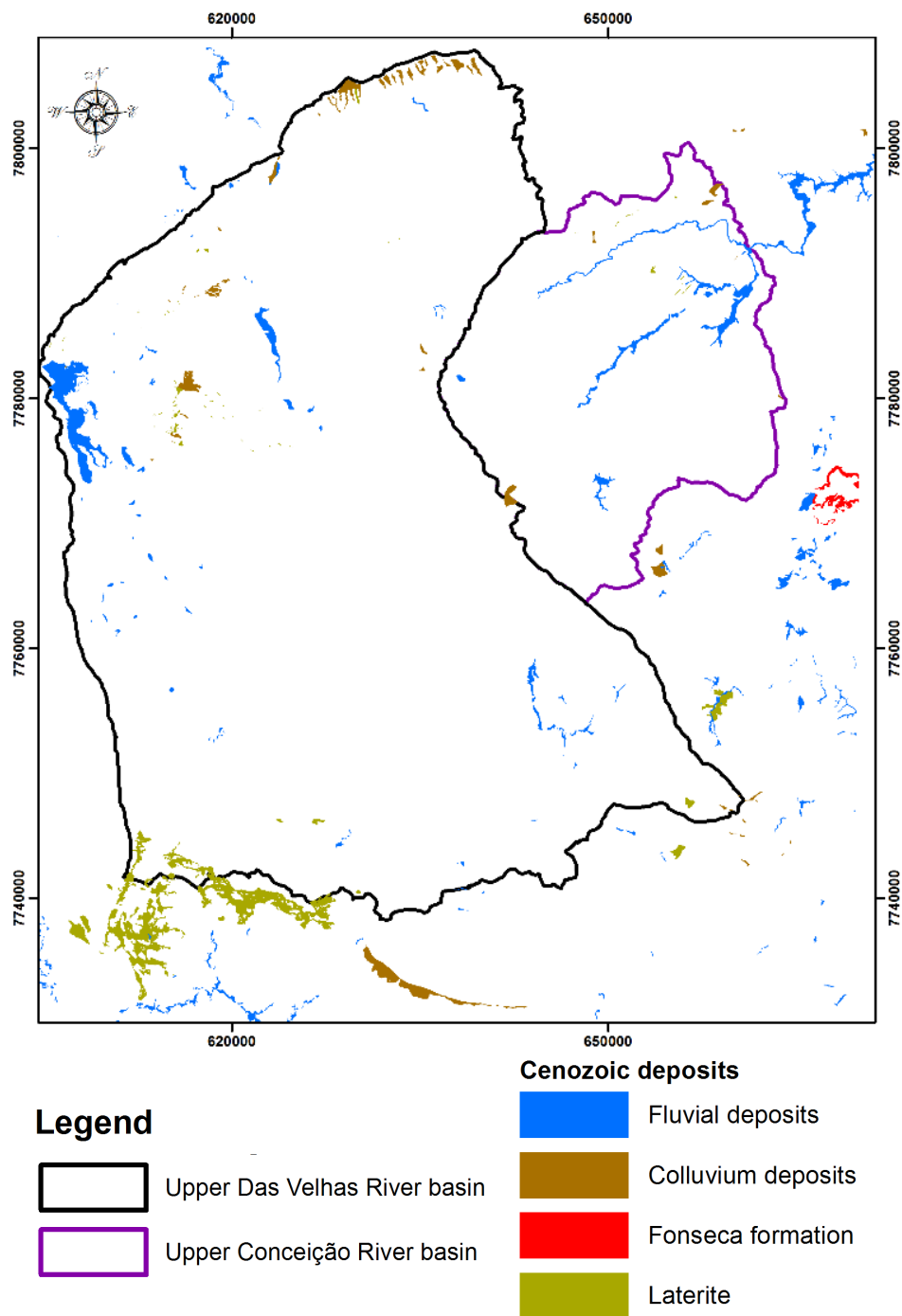


Figure AR4: Spatial distribution of Cenozoic units in the QF, excluding iron duricrusts. Geological data: Lobato et al., 2005. The Fonseca formation refers to Eocene clayey and sandy lacustrine deposits often interpreted as tectonically controlled (e.g., Sant'anna et al., 1997).

References

- Aguilar, C., Alkmim, F.F., Lana, C. and Farina, F.: Palaeoproterozoic assembly of the São Francisco craton, SE Brazil: New insights from U–Pb titanite and monazite dating, *Precambrian Res.*, 289, 95–115, <https://doi.org/10.1016/j.precamres.2016.12.001>, 2017.
- Alkmim, F.F. and Marshak, S.: Transamazonian orogeny in the Southern Sao Francisco craton region, Minas Gerais, Brazil: evidence for Paleoproterozoic collision and collapse in the Quadrilátero Ferrífero, *Precambrian Res.*, 90, 29–58, [https://doi.org/10.1016/S0301-9268\(98\)00032-1](https://doi.org/10.1016/S0301-9268(98)00032-1), 1998.
- Alkmim, F.F. and Martins-Neto, M.A.: Proterozoic first-order sedimentary sequences of the São Francisco craton, eastern Brazil, *Mar. Petrol. Geol.*, 33, 127–139, <https://doi.org/10.1016/j.marpetgeo.2011.08.011>, 2012.
- Alkmim, F. F. and Teixeira, W.: The Paleoproterozoic Mineiro Belt and the Quadrilátero Ferrífero, in: São Francisco Craton, Eastern Brazil: Tectonic Genealogy of a Miniature Continent, edited by: Heilbron, M., Cordani, U. G., and Alkmim, F. F., Springer-Verlag, 71–94, http://dx.doi.org/10.1007/978-3-319-01715-0_5.chapter 5, 2017.
- Almeida, F. F. M., Hasui, Y., de Brito Neves, B. B. and Fuck, R.A.: Brazilian structural provinces: an introduction, *Earth-Sci. Rev.*, 17, 1–29, [https://doi.org/10.1016/0012-8252\(81\)90003-9](https://doi.org/10.1016/0012-8252(81)90003-9), 1981.
- Carmo, I. D. O: Geocronologia do intemperismo Cenozóico no sudeste do Brasil. Ph.D. thesis, Universidade Federal do Rio de Janeiro, Brazil, 134 pp., 2005.
- Chemale Jr, F., Rosière, C.A. and Endo, I.: The tectonic evolution of the Quadrilátero Ferrífero, Minas Gerais, Brazil, *Precambrian Res.*, 65, 25–54. [https://doi.org/10.1016/0301-9268\(94\)90098-1](https://doi.org/10.1016/0301-9268(94)90098-1), 1994.
- Cogné, N., Gallagher, K. and Cobbold, P.R.: Post-rift reactivation of the onshore margin of southeast Brazil: Evidence from apatite (U–Th)/He and fission-track data, *Earth Planet. Sc. Lett.*, 309, 118–130, <https://doi.org/10.1016/j.epsl.2011.06.025>, 2011.
- Cogné, N., Gallagher, K., Cobbold, P.R., Riccomini, C. and Gautheron, C.: Post-breakup tectonics in southeast Brazil from thermochronological data and combined inverse-forward thermal history modeling, *J. Geophys. Res.-Sol. Ea.*, 117, 1–16, <https://doi.org/10.1029/2012JB009340>, 2012.
- Endo, I. and Fonseca, M.A.: Sistema de cisalhamento Fundão-Cambotas no Quadrilátero Ferrífero, MG: geometria e cinemática, *Revista da Escola de Minas*, 45, 28–31, 1992.
- Engelmann de Oliveira, C.H.E., Jelinek, A.R., Chemale Jr, F. and Cupertino, J.A.: Thermotectonic history of the southeastern Brazilian margin: Evidence from apatite fission track data of the offshore Santos Basin and continental basement, *Tectonophysics*, 685, 21–34, <https://doi.org/10.1016/j.tecto.2016.07.012>, 2016.
- Farina, F., Albert, C., Dopico, C.M., Gil, C.A., Moreira, H., Hippertt, J.P., Cutts, K., Alkmim, F.F.D. and Lana, C.: The Archean–Paleoproterozoic evolution of the Quadrilátero Ferrífero (Brasil): Current models and open questions, *J. S. Am. Earth Sci.*, 68, 4–21, <https://doi.org/10.1016/j.jsames.2015.10.015>, 2016.

- Fonseca, A.C.L., Piffer, G.V., Nachtergaele, S., Van Ranst, G., De Grave, J. and Novo, T.A.: Devonian to Permian post-orogenic denudation of the Brasília Belt of West Gondwana: insights from apatite fission track thermochronology, *J. Geodyn.*, 1–14, <https://doi.org/10.1016/j.jog.2020.101733>, 2020.
- Gallagher, K., Hawkesworth, C.J. and Mantovani, M.S.M.: The denudation history of the onshore continental margin of SE Brazil inferred from apatite fission track data, *J. Geophys. Res.-Sol. Ea.*, 99, 117–145, <https://doi.org/10.1029/94JB00661>, 1994.
- Heilbron, M., Cordani, U.G. and Alkmim, F.F. (Eds.): São Francisco Craton, Eastern Brazil: Tectonic Genealogy of a Miniature Continent, Springer-Verlag, 2017.
- Hiruma, S.T., Riccomini, C., Modenesi-Gauttieri, M.C., Hackspacher, P.C., Neto, J.C.H. and Franco-Magalhães, A.O.: Denudation history of the Bocaina Plateau, Serra do Mar, southeastern Brazil: Relationships to Gondwana breakup and passive margin development, *Gondwana Res.*, 18, 674–687, <https://doi.org/10.1016/j.gr.2010.03.001>, 2010.
- Jelinek, A.R., Chemale Jr, F., Van der Beek, P.A., Guadagnin, F., Cupertino, J.A. and Viana, A.: Denudation history and landscape evolution of the northern East-Brazilian continental margin from apatite fission-track thermochronology, *J. S. Am. Earth Sci.*, 54, 158–181, <https://doi.org/10.1016/j.jsames.2014.06.001>, 2014.
- Krob, F.C., Glasmacher, U.A., Karl, M., Perner, M., Hackspacher, P.C. and Stockli, D.F.: Multi-chronometer thermochronological modelling of the Late Neoproterozoic to recent tT-evolution of the SE coastal region of Brazil, *J. S. Am. Earth Sci.*, 92, 77–94, <https://doi.org/10.1016/j.jsames.2019.02.012>, 2019.
- Lobato, L.M.; Baltazar, O.F.; Reis, L.B.; Achtschin, A.B.; Baars, F.J.; Timbó, M.A.; Berni, G.V; Mendonça, B.R.V. de; and Ferreira, D.V: Projeto Geologia do Quadrilátero Ferrífero - Integração e Correção Cartográfica em SIG com Nota Explicativa, CODEMIG, Belo Horizonte, 2005.
- Saadi, A., Sgarbi, G.N.C. and Rosière, C.A.: A Bacia do Gongo Soco; nova bacia terciária no Quadrilátero Ferrífero: controle cárstico e/ou tectônico, in: *Proceedings of the 37th Congresso Brasileiro de Geologia*, São Paulo, 600–601, 1992.
- Sant’Anna, L.G., Schorscher, H.D. and Riccomini, C.: Cenozoic tectonics of the Fonseca basin region, eastern Quadrilátero Ferrífero, MG, Brazil, *J. S. Am. Earth Sci.*, 10, 275–284, [https://doi.org/10.1016/S0895-9811\(97\)00016-3](https://doi.org/10.1016/S0895-9811(97)00016-3), 1997.
- Tello Saenz, C.T., Neto, J.H., Iunes, P.J., Guedes, S., Hackspacher, P.C., Ribeiro, L.F.B. and Paulo, S.R.: Thermochronology of the South American platform in the state of São Paulo, Brazil, through apatite fission tracks, *Radiat. Meas.*, 39, 635–640, <https://doi.org/10.1016/j.radmeas.2004.08.005>, 2005.
- van Ranst, G., Pedrosa-Soares, A.C., Novo, T., Vermeesch, P. and De Grave, J.: New insights from low-temperature thermochronology into the tectonic and geomorphologic evolution of the south-eastern Brazilian highlands and passive margin, *Geosci. Front.*, 11, 303–324, <https://doi.org/10.1016/j.gsf.2019.05.011>, 2020.

Zondervan, J.R., Stokes, M., Boulton, S.J., Telfer, M.W. and Mather, A.E.: Rock strength and structural controls on fluvial erodibility: Implications for drainage divide mobility in a collisional mountain belt, *Earth Planet. Sc. Lett.*, 538, 1-13, <https://doi.org/10.1016/j.epsl.2020.116221>, 2020.

Response to EC1: Interactive comment on "Growing topography due to contrasting rock types in a tectonically dead landscape" by Daniel Peifer et al.

Daniel Peifer et al.

peiferdaniel@gmail.com

Response to EC1

1. Review of 'Growing topography due to contrasting rock types in a tectonically dead landscape' by Peifer et al An interesting and worthy topic of interest to the journal. The paper is of interest to both field workers and modellers. It pulls together, geology, climate and hydrology to unravel a well-understood concept and reverse the thinking. It is particularly interesting in that it presents an alternative view of denudation and relief. What is particular pleasing is an examination of the geology and geomorphology of a stable or dead landscape system. The paper is clearly written with an extensive list of references. The Abstract summarises the paper well.

Dear Greg Hancock,

Thank you very much for your encouraging and thoughtful comments. We are delighted that your evaluation of our contribution is positive. We would also like to thank you for conducting such a helpful review process, particularly during the pandemic.

2. Some suggestions. In regards to the area-slope analysis and profile analysis, some extra detail and analysis may be extracted from Cohen et al (JGR, 2008 doi:10.1029/2007JF000820).

Thank you for this suggestion. However, in our contribution, we have not used an area-slope method, relying instead on the upstream integrated area (chi) transform approach. Given this, we have not carried out any additional experiments in light of this suggestion. If the editor has some specific extra analysis he would like to see, then we would welcome them.

3. *It is not clear what you mean by (line 376) 'Given the long period since the cessation of crustal thickening, we conjecture that the landscape has not achieved equilibrium and that equilibrium is not a natural attractor in ancient landscapes. Our results indicate that the fluvial erosion efficiency differs by three orders of magnitude in the study area, varying as a function of rock type.'* and implications throughout the text. *Is this not captured by the term declining equilibrium? The case for declining equilibrium has been argued by many at other sites globally.*

Thank you for this remark. For improving its clarity, we modified our conclusion to [lines 396-409]: *"We present ^{10}Be concentrations in river sand from catchments spanning the range in topographic metrics and bedrock erodibility in a humid subtropical, tectonically inactive landscape in Brazil. The results of this study suggest that the post-orogenic history of the study area is not a progressive reduction in relief and denudation rates. Instead, the exposure at the surface of rocks with strong lateral contrasts in erodibility amplifies spatial differences in topographic forms and denudation rates over time, sustaining or, indeed, increasing relief in a tectonically dead landscape. Spatial variations in topographic relief and channel steepness are explained by changes in rock type in the study area, and yet denudation rates are not spatially uniform. Contrasts in rock type continue to drive differences in denudation rates in a decaying mountain belt evolving over the Myr timescale, indicating that the landscape has not achieved equilibrium. This study demonstrates that lateral variations in rock strength play an essential role in the dynamics of an ancient mountain belt, and likely in other post-orogenic settings characterised by spatial heterogeneity in lithology. Such lithological heterogeneity controls the tempo and style of landscape response to changes in boundary conditions while also affecting the pattern of landscape denudation."*

About your question, our point is that denudation rates in an ancient mountain belt where the last phase of tectonic activity ended ~500-450 Myr ago vary spatially (by more than an order of magnitude) as a function of rock type, which is at odds with a declining equilibrium scenario as interpreted for other post-orogenic landscapes (e.g., Appalachian Mountains: Matmon et al., 2003; Southern Africa: Scharf et al., 2013; Western Ghats: Mandal et al., 2015) where, despite decaying, topographic forms are constant through time, and denudation rates are spatially invariant irrespective of differences in rock type or topographic relief. Please see response 3 to RC1.

4. Minor issue: 'We' and 'our' in the Conclusion is repetitive.

Thanks. We modified the conclusion to overcome this issue.

Additional note:

Dear Editor,

In addition to the changes described in the response letters, we have made several small revisions to clarify points, correct typos, and improve the text's fluency. All these changes are highlighted in the version of the manuscript with tracked changes.

Sincerely,

Daniel

References

Mandal, S.K., Lupker, M., Burg, J.P., Valla, P.G., Haghipour, N. and Christl, M.: Spatial variability of ^{10}Be -derived erosion rates across the southern Peninsular Indian escarpment: A key to landscape evolution across passive margins, *Earth Planet. Sc. Lett.*, 425, 154–167, <https://doi.org/10.1016/j.epsl.2015.05.050>, 2015.

Matmon, A., Bierman, P.R., Larsen, J., Southworth, S., Pavich, M. and Caffee, M.: Temporally and spatially uniform rates of erosion in the southern Appalachian Great Smoky Mountains, *Geology*, 31, 155–158, [https://doi.org/10.1130/0091-7613\(2003\)031<0155:TASURO>2.0.CO;2](https://doi.org/10.1130/0091-7613(2003)031<0155:TASURO>2.0.CO;2), 2003.

Scharf, T.E., Codilean, A.T., De Wit, M., Jansen, J.D. and Kubik, P.W.: Strong rocks sustain ancient postorogenic topography in southern Africa, *Geology*, 41, 331–334, <https://doi.org/10.1130/G33806.1>, 2013.

Response to SC1: Interactive comment on "Growing topography due to contrasting rock types in a tectonically dead landscape" by Daniel Peifer et al.

Daniel Peifer et al.

peiferdaniel@gmail.com

Response to SC1

1. Hello, I just read through this and found it to be very interesting - there's not enough attention paid to tectonically dead landscapes. I recently published two papers that you might find to be relevant. I've attached them here. Cheers Manny

Dear Manny Gabet,

Thank you for such an encouraging comment.

It is fascinating that you are interested in the many intriguing questions that tectonically dead landscapes pose, and indeed they deserve more attention. I read your papers on the effects of lithological heterogeneity in the evolution of mountainous topography with enthusiasm; the reading was delightful, and it gave me many insights of future work. Again, thank you very much.

Sincerely,

Daniel Peifer

Growing topography due to contrasting rock types in a tectonically dead landscape

Daniel Peifer^{1,2}, Cristina Persano¹, Martin D. Hurst¹, Paul Bishop¹, Derek Fabel³

¹School of Geographical and Earth Sciences, University of Glasgow, Glasgow, G12 8QQ, UK

5 ²CAPES Foundation, Ministry of Education of Brazil, Brasilia - DF 70040-020, Brazil

³Scottish Universities Environmental Research Centre, East Kilbride, G75 0QF, UK

Correspondence to: Daniel Peifer (peiferdaniel@gmail.com)

Abstract. Many mountain ranges survive in a phase of erosional decay for millions of years (Myr) following the cessation of tectonic activity. Landscape dynamics in these post-orogenic settings have long puzzled geologists due to the expectation that topographic relief should decline with time. Our understanding of how denudation rates, crustal dynamics, bedrock erodibility, climate, and mantle-driven processes interact to dictate the persistence of relief in the absence of ongoing tectonics is incomplete. Here we explore how lateral variations in rock type, ranging from resistant quartzites to less-resistant schists and phyllites and up to the least-resistant gneisses and granitic rocks, have affected rates and patterns of denudation and topographic forms in a humid ~~semitropical~~ subtropical, high-relief, post-orogenic landscape in Brazil where active tectonics ended hundreds of Myr ago. We show that catchment-averaged denudation rates are negatively correlated ~~to~~ with mean values of topographic relief, channel steepness and modern precipitation rates. Denudation instead correlates with inferred bedrock strength, with resistant rocks denuding more slowly relative to more erodible rock units, and suggest that the efficiency of fluvial erosion varies primarily due to these bedrock differences. Variations in erodibility continue to drive contrasts in rates of denudation in a tectonically inactive landscape evolving for hundreds of Myr, suggesting that equilibrium is not a natural attractor state and that relief continues to grow through time. Over the long timescales of post-orogenic development, exposure at the surface of rock types with differential erodibility can become a dominant control on landscape dynamics by producing spatial variations in geomorphic processes and rates, promoting the survival of relief, and determining spatial differences in erosional response timescales long after cessation of mountain building.

1 Introduction

25 The question of how landscapes evolve in the aftermath of mountain building has intrigued geomorphologists since the early stages of the discipline, and classic concepts such as the cycle of erosion (Davis, 1899) and dynamic equilibrium landforms (Hack, 1960) were defined in the context of these post-orogenic landscapes (Bishop, 2007). In particular, reasons for the persistence of high topographic relief in ancient mountain belts for many millions of years (Myr) after crustal thickening ~~has~~ ~~ceased~~ remain enigmatic. We know with a reasonable degree of certainty that net erosion in these landscapes and the resulting rebound of the underlying lithosphere by isostasy are central mechanisms controlling the extended longevity of post-orogenic

30

landforms (Gilchrist and Summerfield, 1990; Bishop and Brown, 1992; Bishop, 2007). However, a range of other factors and interactions play essential roles in the post-orogenic evolution of ancient landscapes, including variations in bedrock incision dynamics (e.g., Baldwin et al., 2003; Egholm et al., 2013), mantle-flow dynamics and its influence on the overlying crust (e.g., Gallen et al., 2013; Liu, 2014), vertical and lateral variations in bedrock erodibility (e.g., Twidale, 1976; Bishop and Goldrick, 2010; Gallen, 2018; Bernard et al., 2019; Vasconcelos et al., 2019), densification of the lower crust and resulting reduction of the buoyancy of the lithosphere (e.g., Blackburn et al., 2018), and tectonic uplift in response to far-field stresses (e.g., Hack, 1982; Quigley et al., 2007).

Examples of ancient mountain belts marked by high elevations and steep slopes include the Appalachian Mountains, several mountain ranges SE Brazil, the Cape Mountains, [parts of the East Australian Highlands](#) ~~the Lachlan Fold Belt in SE Australia~~, the Ural Mountains, the Caledonides, the Western Ghats, and the Sri Lanka orogen (Fig. 1). These high-relief post-orogenic settings are associated with different climate conditions, tectonic histories, effective elastic thicknesses of the lithosphere, and geological architectures. For instance, some of these ancient mountain belts are located in a passive margin context, whereas others are located in the deep interior of the continents (Fig. 1). Yet they share common geomorphic characteristics such as overall low rates of denudation (e.g., Harel et al., 2016), relative Cenozoic tectonic quiescence (e.g., Twidale, 1976; Mandal et al., 2015), exposure of a variety of resistant and more erodible lithologies (e.g., Bishop and Goldrick, 2010; Gallen, 2018; Vasconcelos et al., 2019), peak elevations that may exceed 2000 m and average elevations commonly higher than 1000 m (e.g., Gallen et al., 2013; Scharf et al., 2013; von Blanckenburg et al., 2004).

Early landscape evolution schemes (e.g., Davis, 1899) and quantitative estimates of post-orogenic relief reduction (e.g., Ahnert, 1970; Baldwin et al., 2003; Egholm et al., 2013) predict a progressive decay in both topographic relief and denudation rates, with residual post-orogenic landforms marked by featureless topography reminiscent of peneplains after hundreds of Myr of ongoing denudation. More recently, a range of geomorphic and thermochronologic data indicates that topographic evolution in ancient mountain chains may be more dynamic than otherwise expected, with different types of forcing (e.g., tectonic, climatic, lithologic, mantle-driven) affecting at least some of these landscapes in post-orogenic times (e.g., Pazzaglia and Brandon, 1996; Quigley et al., 2007; Gallen et al., 2013; Tucker and van der Beek, 2013; Liu, 2014; Gallen, 2018). Our current knowledge on post-orogenic landscape evolution suffers from an incomplete understanding of how and to what extent different types of forcing may act in concert in driving the development of decaying mountain belts that are evolving over Myr timescales (Bishop, 2007; Tucker and van der Beek, 2013).

Most post-orogenic landscapes are characterised by complex and spatially variable lithology, often including crystalline rocks, different types of deformed metasediments and sedimentary covers, and volcanic units (e.g., Dorr, 1969; Bierman and Caffee, 2001; Barreto et al., 2013; Gallen et al., 2013; Mandal et al., 2015). Spatial variations in rock type have long been identified as a critical factor in post-orogenic development for they determine spatial heterogeneities in erodibility (e.g., Hack, 1960; Dorr, 1969; Hack, 1975; Twidale, 1976; Mills, 2003; Bishop and Goldrick, 2010; Gallen, 2018; Bernard et al., 2019; Vasconcelos et al., 2019; [Zondervan et al., 2020a](#)). In particular, correlations between rock type and topographic forms were

observed in post-orogenic landscapes, with high topographic relief and steep channel reaches associated with resistant rocks (e.g., Hack, 1960, 1975; Twidale, 1976; Mills, 2003; Spotila et al., 2015; Gallen, 2018), ~~and such links were interpreted in several cases as a dynamic equilibrium adjustment, likely driven by denudational isostatic rebound, where spatial variations in topographic relief persist over time as a function of contrasts in bedrock erodibility and denudation rates are spatially uniform (e.g., Hack, 1960; Matmon et al., 2003; Scharf et al., 2013; Mandal et al., 2015).~~ These observations were interpreted, in several cases, as equilibrium adjustments where spatial variations in rock strength are balanced by variations in topographic relief so that everywhere is eroding at the same rate, with the corollary that topographic forms are constant through time in a 'topographic equilibrium' likely driven by isostatic uplift (e.g., Hack, 1960; Matmon et al., 2003; Scharf et al., 2013; Mandal et al., 2015). In contrast, recent modelling studies indicate that exposure at the surface of rock units with substantial differences in rock strength dictate complex patterns of denudation, with significant spatial and temporal variations in denudation rates and possibly the persistence of non-steady-state conditions as long as different rock units are exposed (Forte et al., 2016; Perne et al., 2017). Post-orogenic settings are well-suited as natural laboratories to explore further the role of spatial variations in lithology in landscape evolution as these are lithologically heterogeneous landscapes that last experienced major active rock uplift tens to hundreds of millions of years ago (Bishop, 2007). Nevertheless, few studies have directly explored the spatial variability of denudation rates in post-orogenic settings as a function of the full spectrum of variations in underlying lithology and topographic relief in these landscapes.

Here, we investigated how denudation rates vary spatially in a humid ~~semitropical~~ subtropical, high-relief post-orogenic area in Brazil where the last phase of tectonic activity ended ~500-450 Myr ago and explored the relationships between denudation rates and topographic relief, channel steepness, precipitation rates and rock type. Denudation rates were measured using ¹⁰Be concentrations in fluvial sediments from catchments spanning the range of topographic relief and bedrock lithologies in the study area.

2 Geological setting

The study area is the Quadrilátero Ferrífero (Brazil), one of Brazil's ~~the~~ highest elevation areas ~~in Brazil~~, with a peak elevation of 2,076 m; located in the continental interior ~350 km away in a straight line from the Atlantic Ocean (Fig. 2). The name Quadrilátero Ferrífero (QF) translates as 'Iron Quadrangle', referring both to its vast iron ore reserves and the roughly rectangular alignment of its ridges (Dorr, 1969). Local relief can reach 1,189 m over a 2-km diameter circular window (Fig. 2A). There is an abundance of mixed bedrock-alluvial channels that incise deeply ~~cut~~ into the most resistant rocks, but are less incised where more erodible lithologies are exposed; everywhere, however, the slope is enough for the detrital material to be removed, as alluvium has not significantly accumulated in the study area (Dorr, 1969). Normalised channel steepness, which is a metric for channel slope normalised to catchment size according to an assumed channel profile concavity, differs over three orders of magnitude (Fig. 2C). The regional climate ranges from Cwa to Cwb in Köppen-Geiger's classification (Alvares

95 [et al., 2013](#)). Mean annual precipitation ~~rates vary~~[ies](#) from 1356 to 1729 mm/yr (Fick and Hijmans, 2017), and the mean annual temperature is $\sim 20^{\circ}\text{C}$ (Dorr, 1969).

Resistant and more erodible lithologies are exposed in a complex geological pattern (Fig. 2B) that reflects a polyphase deformation history, the last episode of which was $\sim 500\text{--}450$ Myr ago (Dorr, 1969; Chemale Jr et al., 1994; Alkmim and Marshak, 1998). ~~The~~ [Exposed](#) lithologies comprise principally Archean and Paleoproterozoic sequences, usually
100 metamorphosed and steeply dipping ($\geq 35^{\circ}$), including gneisses and granitic rocks, schists, phyllites, quartzites, metaconglomerates, metacarbonate rocks, metavolcanics, banded iron formations, and iron duricrusts (Dorr, 1969; Chemale Jr et al., 1994; Alkmim and Marshak, 1998). An array of geochronological data imply that the current topography is long-lived. [These data](#) include: ~~goethite (U-Th)/He ages and cosmogenic ^3He concentrations indicating laterite development since 55 Ma (Monteiro et al., 2018); 70 Ma $^{40}\text{Ar}/^{39}\text{Ar}$ ages in weathering profiles (Vasconcelos and Carmo, 2018)~~ [a relatively large set of \(U-Th\)/He data \(\$n = 291\$ \) and cosmogenic \$^3\text{He}\$ concentrations \(\$n = 71\$ \) in iron oxides showing mineral precipitation ages as old as 55 Ma \(varying from \$55.3 \pm 5.5\$ to \$0.4 \pm 0.1\$ Ma\), and exposure ages ranging from \$10.9 \pm 1.2\$ to \$0.2 \pm 0.1\$ Ma, with age versus elevation relationships suggesting older ages and a more extended history of exposure in iron duricrust-covered plateaus at higher elevations \(Monteiro et al., 2014, 2018\); \$^{40}\text{Ar}/^{39}\text{Ar}\$ dating of Mn oxide grains collected in nine weathering profiles in the QF \(\$n = 174\$ grains that produced reliable results\) yielding ages ranging from \$94.6 \pm 5.5\$ to \$12.3 \pm 0.5\$ Ma, yet](#)
105 [predominantly distributed between 30–60 Ma \(Spier et al., 2006; Vasconcelos and Carmo, 2018\)](#); and low denudation rates (< 3 m/Myr) ~~inferred~~ [implied](#) by cosmogenic ^3He and ^{10}Be inventories (Monteiro et al., 2018; Salgado et al., 2008). However, some authors [have](#) hypothesised, [based principally on the post-depositional deformation of Cenozoic sediments that fill small basins \(Fig. S1\)](#), that the eastern part of the QF was affected by Cenozoic tectonics ~~based principally on field evidence of post-depositional deformation in Cenozoic units that fill small basins~~ (e.g., Sant'anna et al., 1997).

115 3 Methods

3.1 Determination of denudation rates

We collected alluvial sand from the bed of 25 active channels [for the determination of denudation rates from detrital \$^{10}\text{Be}\$ concentrations. Sampling included](#) catchments spanning the range of topographic relief in the QF (Fig. 2A) and the range of bedrock lithologies (Fig. 2B), from ~~the~~ resistant quartzites to the least-resistant (under humid ~~semitropical~~ [subtropical](#)
120 conditions) gneisses and granitic rocks, ~~for the determination of denudation rates from detrital ^{10}Be concentrations~~. The sampled basins do not show evidence of deep-seated landslides, and there are no records of significant landslide activity in the study area (Dorr, 1969). Samples were prepared and analysed at SUERC (Scottish Universities Environmental Research Centre), Scotland, following standard procedures (Kohl and Nishiizumi, 1992); NIST SRM4325 was the ^{10}Be standard. The resulting $^{10}\text{Be}/^9\text{Be}$ ratios for each sample were corrected for processed blank ratios ($n = 2$), ranging between 0.2 and 3.2% of
125 the sample $^{10}\text{Be}/^9\text{Be}$ ratios, with uncertainties propagated in quadrature (Balco et al., 2008).

Catchment-averaged denudation rates were derived from ^{10}Be concentrations using the CRONUS online calculator v. 3.0 (Balco et al., 2008). We used the CAIRN method (Mudd et al., 2016) to quantify catchment-averaged pressure employing a pixel-by-pixel approach and recommended parameters (Mudd et al., 2016). We report denudation rates using the time-independent Lal/Stone scaling method (Lal, 1991; Stone, 2000), and assuming a standard bedrock density of 2.7 g/cm^3 (e.g., von Blanckenburg et al., 2004; Mandal et al., 2015). We have not applied corrections for topographic shielding (DiBiase, 2018). We have also incorporated eight detrital ^{10}Be -derived concentration measurements previously published for the QF (Salgado et al., 2008) in our dataset; however, we recalculated denudation rates using the ~~same~~ method described above to ensure consistency (Table S1).

3.2 Quantification of catchment-averaged geomorphic metrics

We used a 12 m TanDEM-X (TerraSAR-X add-on for Digital Elevation Measurement) DEM to extract the topographic metrics (i) local relief, and (ii) normalised channel steepness. The WordClim v.2 dataset (Fick and Hijmans, 2017) was used to extract (iii) mean annual precipitation rates. These metrics have been demonstrated to play an essential role in revealing the pattern and style of landscape evolution in erosive settings (e.g., Ahnert, 1970; Montgomery and Brandon, 2002; DiBiase et al., 2010; Portenga and Bierman, 2011; Harel et al., 2016). Catchments were extracted from the DEM following standard hydrological routing procedures using sample locations as pour points. Catchment-averaged values for each metric were determined as the average of all local values within each catchment.

Various authors [have](#) observed empirically that channel slope (S) declines progressively as contributing drainage area (A) increases in the downstream direction of a channel profile, in a relationship that can be described by a power-law (e.g., Flint, 1974):

$$S = k_s A^{-\theta}, \quad (1)$$

where θ , termed the '[channel](#) concavity', ~~index~~, controls how rapidly channel slope decreases with increasing drainage area, and k_s , referred to as the '[channel](#) steepness', ~~index~~, is a measure of channel steepness normalised by upstream drainage area which has been demonstrated to correlate positively with denudation rates in different geomorphic conditions (e.g., DiBiase et al., 2010; Mandal et al., 2015; Harel et al., 2016). The parameters k_s and θ covary, and this autocorrelation is corrected by defining a fixed reference concavity ~~index~~ (θ_{ref}) which is used to extract a normalised [channel](#) steepness ~~index~~ (k_{sn}) from the data (Kirby and Whipple, 2012).

~~The~~ Eq. (1) can be used to derive estimates of k_s and θ (or k_{sn}) from regressions of log-transformed slope-area data (Kirby and Whipple, 2012). Alternatively, one can extract k_{sn} using an approach referred to as the integral method (Perron and Royden, 2013). For that, the Eq. (1) is rearranged replacing S ~~for~~ [with](#) dz/dx and separating these variables, where z is elevation and x is distance along the channel, which is then integrated in the upstream direction from an arbitrarily base level at x_b , resulting in an equation for the elevation profile (e.g., Mudd et al., 2018):

$$z(x) = z(x_b) + \left(\frac{k_s}{A_0^\theta}\right) \int_{x_b}^x \left(\frac{A_0}{A(x)}\right)^\theta dx, \quad (2)$$

where A_0 is a reference drainage area that is inserted to make the area term dimensionless (Perron and Royden, 2013). One can then define a longitudinal coordinate chi (χ) with dimensions of length using (Perron and Royden, 2013; Mudd et al., 2014):

$$\chi = \int_{x_b}^x \left(\frac{A_0}{A(x)}\right)^\theta dx. \quad (3)$$

In the case of $A_0 = 1$, the slope of a longitudinal profile in a z versus χ plot is the channel steepness ~~index~~ (k_s), or the normalised [channel](#) steepness ~~index~~ (k_{sn}) if the extraction is based on θ_{ref} . We quantified k_{sn} as the derivative of χ and z (e.g., Mudd et al., 2014) instead of using regressions of slope-area data (e.g., DiBiase et al., 2010; Kirby and Whipple, 2012) because the integral method does not require estimating slope from the DEM, resulting in more precise k_{sn} values (Perron and Royden, 2013). We estimated how θ varies over the study area based on the disorder method (Hergarten et al., 2016), which was carried out using routines developed by Mudd et al. (2018), to derive an optimal θ value for the entire landscape. The drainage network was extracted using an area threshold of 0.5 km² (e.g., Beeson et al., 2017; Campforts et al., 2020), which is lower than the minimum drainage area among the catchments where we collected fluvial sediments (0.86 km²), and is a reasonable critical threshold for the study area (Fig. S42). We computed θ for all catchments of stream-order higher than third-order following Strahler (1957) ($n = 144$), covering the entire study area, that were extracted using code developed by Clubb et al. (2019). The mean θ for the QF (0.44; Table 1) is close to the frequently used value of 0.45 (e.g., Mandal et al., 2015), thus we set 0.45 as the reference concavity from which we computed the normalised channel steepness employing the segmentation method of Mudd et al. (2014).

We quantified local relief as the elevation range within a neighbourhood defined by a 2-km diameter circular window. The choice of the local relief window was based on sensitivity analysis (DiBiase et al., 2010). We compared the goodness-of-fit in bivariate regressions between average values of local relief (with window diameter varying from 0.5 to 5.0 km) and normalised channel steepness for every catchment in the study area with stream-order higher than second-order. In this situation, the local relief obtained using the 2-km diameter window exhibits the highest goodness-of-fit (measured using the ordinary least squares method; Myers, 1990) with catchment-averaged normalised channel steepness (Fig. S23) and, therefore, it is the one that has been used throughout. Finally, we extracted mean annual precipitation rates from the 30 arc-second spatial resolution WorldClim v.2 global monthly precipitation dataset for the years 1970 to 2000, which is based on raw weather station data and covariates from satellite sensors that were interpolated and combined, creating global climate surfaces (Fick and Hijmans, 2017).

3.3 Lithological strength and fluvial erosion efficiency in the QF

The QF is characterised by the presence of vast ore deposits, particularly gold, iron, and manganese (Dorr, 1969; Lobato et al., 2001). The exploitation of these ore reserves has led to focused research, and the QF is the most systematically investigated

geological domain of Brazil (Lobato et al., 2001). We extracted geological data from the 'Projeto Geologia do Quadrilátero Ferrífero' dataset mapped at a scale of 1:25,000 (Lobato et al., 2005).

Rivers in the study area erode through a landscape marked by variations in rock type, including granitic, argillaceous, quartzose, and carbonate rocks, as well as iron formations. These rock units are metamorphosed and steeply dipping as a result of QF's polyphase deformation history (Dorr, 1969; Chemale Jr et al., 1994; Alkmim and Marshak, 1998). There is a clear consensus from geological research that the exposed lithologies have differential resistance to weathering and erosion, whereby quartzites, banded iron formations, and iron duricrusts comprise the most resistant lithologies; schists, phyllites, dolomitic units, and metavolcanics rocks are less-resistant lithologies; and gneisses and granitic rocks are the least-resistant rocks exposed in the QF (e.g., Dorr, 1969; Salgado et al., 2008; Monteiro et al., 2018; Vasconcelos and Carmo, 2018). Following the approach taken by previous studies (e.g., Lague et al., 2000; Korup, 2008; Jansen et al., 2010; Hurst et al., 2013), we assumed that such classification of rock strength as a function of rock type is valid although we do not have rock strength measurements to support it. Given the humid ~~semitropical~~ subtropical condition of the QF, we expect differential resistance to reflect variations in the susceptibility to chemical weathering of the different rock units (Meybeck, 1987; White and Blum, 1995). For instance, gneisses and granitic rocks with an abundant presence of feldspars are readily weathered whereas physically robust and chemically inert quartzites weather much ~~slower~~ more slowly, via the intergranular solution of quartz (Dorr, 1969). In general, in the study area, quartzites and banded iron formations form pronounced ridges and steep landforms with relatively unweathered outcrops compared to areas in gneisses and granitic rocks associated with broad lowlands that are deeply weathered, with regoliths extending to depths of 50 m or more (e.g. Dorr et al., 1969; Salgado et al., 2008).

Theory and field observations demonstrate that rock strength influences long-term fluvial incision rates in erosive settings (e.g., Gilbert, 1877; Howard and Kerby, 1983; Stock and Montgomery, 1999; Whipple and Tucker, 1999; Jansen et al., 2010; Bursztyn et al., 2015) in concert with a number of other controls, including climate conditions and runoff efficiency, channel width scaling, extreme hydrologic events, and frequency of debris-flow (e.g., Snyder et al., 2000; Whipple et al., 2000a; Kirby and Whipple, 2001; Duvall et al., 2004; Zondervan et al., ~~2019~~ 2020b). All these factors are encapsulated in a dimensional coefficient of erosion efficiency (K) in the commonly used stream-power model (Howard and Kerby, 1983):

$$E = KA^mS^n, \tag{4}$$

where E is the long-term fluvial erosion, A is the upstream contributing drainage area, S is the local channel gradient, and m and n are positive exponents that depend on incision process, channel hydraulics, and rainfall variability (Whipple and Tucker, 1999).

Whereas most variables in the stream-power model can be derived from DEM data, the fluvial erosion efficiency coefficient (K) cannot be measured directly, and thus computing K demands constraints on timing/rates of river evolution (Zondervan et al., ~~2019~~ 2020b). We have a limited understanding of how K varies in different geomorphic conditions and what controls its variability due to the few studies that derived absolute constraints on K and confounding between the multiple controls encoded

in K (Snyder et al., 2000; Whipple et al., 2000a; Duvall et al., 2004; Harel et al., 2016; Zondervan et al., 2019, 2020b). More sophisticated versions of the stream-power model may explicitly account for different controls in K (e.g., DiBiase and Whipple, 2011; Zondervan et al., 2019; Campforts et al., 2020; Zondervan et al., 2020b), yet such approach requires specific data on of an adequate resolution such as river hydraulic geometry, rock strength measurements, and hydrological data to resolve spatial and temporal runoff variability, which are not readily available.

We computed catchment-averaged values of K for the QF using an approach similar to Gallen (2018) based on k_{sn} and average erosion rates. Such an approach requires that spatial variability in long-term rock uplift over the study area is low, which is a reasonable assumption for the QF. Rearranging Eq. (4) to solve for channel slope can cast the stream-power model in the same form as Eq. (1):

$$S = \left(\frac{E}{K}\right)^{1/n} A^{-m/n}, \quad (5a)$$

where:

$$k_{sn} = \left(\frac{E}{K}\right)^{1/n}, \quad (5b)$$

$$\theta_{ref} = m/n, \quad (5c)$$

and thus:

$$E = K k_{sn}^n. \quad (5d)$$

We extracted k_{sn} using 0.45 as the reference concavity which, assuming $m = 0.45$ and $n = 1$, and hence yields derived K values with have units of $\text{m}^{0.1}/\text{yr}$. We assumed that catchment-wide denudation rates derived from detrital ^{10}Be concentrations are representative for of long-term fluvial incision in the QF, considering that there are no records of occurrence of deep-seated landslides (Dorr, 1969) and sampled catchments are of a reasonable size. We calculated K assuming $n = 1$ and $n = 2$, which have been previously demonstrated as feasible values of n (Lague, 2014). In the study area, the range in precipitation rates is relatively low (from 1356 to 1729 mm/yr), with areas in higher elevations principally underlain by resistant rocks receiving more precipitation than valley bottoms in more erodible rock units (Fig. S34), indicating opposing effects in K between inferred rock strength and precipitation rates. We explored how rock type and precipitation rates are linked to catchment-averaged values of K .

4 Results

4.1 Catchment-averaged denudation rates in the QF

Catchment-averaged denudation rates in the study area range from 0.6 ± 0.1 m/Myr to 22.2 ± 1.9 m/Myr, with a regional mean denudation rate of 6.4 m/Myr (Fig. 3; Table S1). Denudation rates in the QF are thus comparable to or lower than previous

estimates of denudation rates in other tectonically inactive, post-orogenic settings (e.g., Harel et al., 2016), including the Cape Mountains (e.g., Scharf et al., 2013), the Appalachian Mountains (e.g., Matmon et al., 2003), the Ozark dome (e.g., Beeson et al., 2017), the Sri Lankan uplands (e.g., von Blanckenburg et al., 2004), and the Western Ghats (e.g., Mandal et al., 2015).

250 However, denudation rates are not uniformly low in the study area, ~~but vary~~ varying by more than ~~one~~ an order of magnitude ~~in the study area~~ (Fig. 3), from the slowly denuding catchments in the eastern part of the QF, where all catchments exhibit denudation rates lower than 3.5 m/Myr, to the western part of the QF where catchments ~~denude~~ are eroding at higher rates up to 22.2 ± 1.9 m/Myr (Fig. 3).

4.2 Links between topographic metrics, precipitation rates, rock type, and denudation rates

255 We find that catchment-averaged denudation rates are negatively correlated with mean values of local ~~catchment-averaged~~ relief (Fig. 4A), contrary to the established understanding of links between denudation and topographic relief, and the bulk of supporting empirical studies (e.g., Ahnert, 1970; Montgomery and Brandon, 2002; DiBiase et al., 2010; Harel et al., 2016). Similarly, catchment-averaged denudation rates are negatively correlated with mean values of normalised channel steepness (Fig. 4B), ~~which is a parameter~~ often used to infer denudation rates based on the empirical ~~evidence for a~~ positive correlation
260 between denudation and normalised channel steepness in tectonically active landscapes (e.g., DiBiase et al., 2010; Kirby and Whipple, 2012; Harel et al., 2016). We also find a negative relationship between catchment-averaged denudation rates and mean annual precipitation (Fig. 4C), contrary to the expectation that wetter climates drive more rapid denudation (e.g., Moon et al., 2011; Harel et al., 2016) and, finally, a weak correlation between catchment-averaged denudation rates and ~~with~~ catchment area (Fig. S45). However, we observe that catchment-averaged denudation rates may increase together with mean
265 values of topographic metrics and precipitation rates for individual rock types, although with such small sample sizes no such relationships are statistically significant at the $\alpha = 0.05$ level except for catchments in phyllites (Fig. 4, S6).

Denudation rates can instead be linked to inferred rock strength (Fig. 4E). Catchments underlain by quartzites are associated with the slowest denudation rates (from 0.6 ± 0.1 to 3.3 ± 0.3 m/Myr, with a mean of 2.2 m/Myr). Catchments in mixed lithologies where $\geq 60\%$ of catchment area consists of resistant lithologies are denuding at slightly higher rates up to 3.5 ± 0.3
270 m/Myr (with a mean of 2.6 m/Myr). In contrast, catchments in less-resistant schists or mixed lithologies with $< 60\%$ of resistant lithologies denude more rapidly. Finally, the low-relief catchments underlain by the least-resistant (under humid ~~semitropical~~ subtropical climate conditions) gneisses and granitic rocks, as well as catchments dominated by phyllites, denude at ~~faster~~ higher rates of up to 22.2 ± 1.9 m/Myr. Similarly, we observe that a higher percentage contribution of resistant rocks in within the catchment area (i.e., areas in quartzites and banded iron formations) determines lower rates of denudation (Fig. 4D).

275 The regional distribution of topographic metrics indicates a positive correlation between topography and inferred rock strength (Fig. 5). In this situation, the high-end of the distribution of topographic metrics, as well as mean and median values, exhibit similar trends of high values for areas underlain by quartzites and banded iron formations, intermediate values for less-resistant rock types such as metabasalts, schists, and phyllites, and low values for areas underlain by the least-resistant basement rocks

which are also marked by lower variability in topography than areas dominated by resistant rocks. However, the low-end of the distribution of topographic metrics shows comparably low values for every rock type, which indicates that subdued local relief and channel steepness occur on all lithologies areas marked by subdued local relief and channel steepness are ubiquitous to all lithologies. We also find positive relationships between catchment-averaged topographic relief and inferred rock strength (Fig. 5C). In particular, we observe that catchments in mixed lithologies where $\geq 60\%$ of catchment area consists of resistant lithologies exhibit substantially higher local relief than catchments in mixed lithologies with less than 60% of resistant lithologies.

4.3 Fluvial erosion efficiency and its relationships with rock type and precipitation rates

Assuming the slope exponent $n = 1$, we find that the fluvial erosion efficiency coefficient (K) differs by three orders of magnitude in the study area, varying from 5.8×10^{-9} to $1.7 \times 10^{-6} \text{ m}^{0.1}/\text{yr}$, with a global mean of $3.3 \times 10^{-7} \text{ m}^{0.1}/\text{yr}$ and a standard deviation of $4.5 \times 10^{-7} \text{ m}^{0.1}/\text{yr}$ (Fig. 6; Table S1). Our results indicate that K decreases substantially with increasing inferred rock strength, varying from low K values in areas underlain by quartzites (with a mean K of $3.6 \times 10^{-8} \text{ m}^{0.1}/\text{yr}$) to considerably higher K values in areas in gneisses and granitic rocks (with a mean K of $1.2 \times 10^{-6} \text{ m}^{0.1}/\text{yr}$) (Fig. 6). We observe some degree of overlap between K values for catchments consisting of different rock types (Fig. 6). However, a Kruskal-Wallis test shows that K is statistically different in catchments underlain by different rock types at the $\alpha = 0.01$ significance level. When the slope exponent n is equal to 2, we find absolute values of K to be more than one order of magnitude lower for every catchment (assuming $m = 0.9$ and $n = 2$, derived values of K have units of $\text{m}^{-0.8}/\text{yr}$). Nevertheless, the same relationship with rock type as the observed for the case of n equal to 1 emerges, with low values of K associated with quartzites and orders of magnitude higher K values in areas in gneisses and granitic rocks (Fig. 6). Finally, although the spatial variability in rainfall is limited in the study area, we observe that catchments that receive more precipitation (in higher elevations underlain by resistant rocks) are associated with substantially lower K values than areas that receive less precipitation (in more erodible rock units) (Fig. S57).

5 Discussion

5.1 Equilibrium as a natural attractor state in a decaying mountain belt

Our results show that bedrock strength controls the variability in topographic relief and channel steepness in the QF. This conclusion is consistent with the classic geomorphic expectation that, all else being equal, terrains underlain by resistant rocks will develop higher topographic relief and steeper channel gradients (e.g., Gilbert, 1877; Hack, 1960; Jansen et al., 2010; Bursztyn et al., 2015). Such correlation between topographic forms and rock strength is the same as that expected in an equilibrium adjustment scenario for a tectonically stable erosive landscape evolving over Myr timescales (Hack, 1960; Montgomery, 2001). In the case of a spatially variable lithological configuration, theory predicts that more erodible rock units are progressively eroded whereas resistant rocks stand proud in relief, up to a point where differential topographic steepness

310 everywhere balances spatial variations in rock strength and denudation rates are then spatially invariant (Hack, 1960). Our
detrital cosmogenic-derived results, however, demonstrate that rates of denudation are kept spatially variable by the exposure
at the surface of different rock types in a tectonically inactive landscape evolving for hundreds of Myr. The landscape has not
achieved any equilibrium or steady-state. We interpret our findings as an indication that ~~quasi~~-equilibrium is likely not a natural
315 heterogeneity (such as the one observed in the study area) is maintained, a conclusion that is consistent with the modelling
results of Forte et al. (2016).

5.2 Lateral variations in rock type as a dominant control on denudation rates and topographic forms in a post-orogenic landscape

Our results suggest that the fluvial erosion efficiency coefficient (K) varies as a function of rock type in the study area, with
320 low K values in resistant units and orders of magnitude higher K values in more erodible rocks. In contrast, we find that spatial
gradients in precipitation rates do not control changes in K in the study area, considering that wetter climate conditions are
generally associated with ~~dietate~~ higher values of K (e.g., Ferrier et al., 2013). However, the fluvial erosion efficiency
coefficient (K) as calculated here incorporates other effects besides rock strength and precipitation rates, such as channel
hydraulic geometry and sediment load (e.g., Snyder et al., 2000; Duvall et al., 2004; Zondervan et al., ~~2019~~ 2020b). Whereas
325 in the Appalachians effects on fluvial erosional efficiency such as channel width and sediment load have been shown to vary
as a function of rock type (e.g., Spotila et al., 2015), we do not have data on such variables for the QF, which is a limitation to
our reasonable interpretation that rock type controls K in the study area. We note, however, that rock strength varies within
each rock type in the study area and, for instance, thin-bedded quartzites with large quantities of muscovite and sericite weather
and erode much ~~easier~~ more easily than average while some granitic areas stand bold in relief where these rocks are coarser-
330 grained and more massive (Dorr, 1969).

The negative relationships we find between ^{10}Be -derived catchment-averaged denudation rates ~~with and catchment-averaged~~
values of topographic relief, channel steepness and precipitation rates, ~~appear to be contradictory to established theory,~~
~~empirical studies and common sense (e.g., Ahnert, 1970; Montgomery and Brandon, 2002; Portenga and Bierman, 2011; Harel~~
~~et al., 2016)~~ are counter-intuitive. However, ~~Yet~~ such relationships are consistent with the stream-power model if one accounts
335 for the magnitude of variations in the fluvial erosion efficiency coefficient (K) estimated for the study area. Our findings ~~are~~
~~in agreement~~ with studies that demonstrated that the link between denudation rates and channel steepness is obscure in settings
where lateral variations in rock strength are important (e.g., Cyr et al., 2014; Campforts et al., 2020), and that a modified
version of the stream-power model including variations in rock strength should be adopted for better predicting spatial patterns
of channel incision (Campforts et al., 2020). Our results imply that modelling studies attempting to reconstruct uplift histories
340 from river profile morphology assuming uniform fluvial erosion efficiency over large areas (e.g., Roberts and White, 2010)
are likely to lead to be flawed ~~results~~, at least in post-orogenic settings.

To compare ~~how~~ our constraints on the fluvial erosion efficiency coefficient ~~stand to~~ with published estimates of K , we also calculate K in units of $\text{m}^{0.2}/\text{yr}$, as reported in several studies (e.g., Stock and Montgomery, 1999; Whipple et al., 2000b; Kirby and Whipple, 2001). We find that the resulting estimates of K in the QF (regional mean K value of $7.1 \times 10^{-7} \text{ m}^{0.2}/\text{yr}$, assuming
345 the slope exponent $n = 1$) are comparable to ~~the low-end~~ or ~~are~~ lower than the low-end of the K values reported by Stock and Montgomery (1999) for a post-orogenic landscape underlain by granites and metasedimentary rocks in humid subtropical Australia (Fig. 7). Similarly, our estimates of K (in Fig. 6) are comparable to ~~the low-end~~ or ~~are~~ lower than the low-end of the K values estimated in crystalline and metamorphic rocks in the Upper Tennessee River (mean K values of $\sim 5 \times 10^{-7} \text{ m}^{0.1}/\text{yr}$; Gallen, 2018), as well as in different physiographic provinces in the Appalachians such as the Blue Ridge (reported K values:
350 $7.8\text{-}3.0 \times 10^{-7} \text{ m}^{0.1}/\text{yr}$; Gallen et al., 2013) and the Valley and Ridge (reported K values: $2.1\text{-}1.5 \times 10^{-6} \text{ m}^{0.1}/\text{yr}$; Miller et al., 2013). In contrast, our results are orders of magnitude lower than estimates of K in tectonically active areas in Hawaii (tropical rainforest climate), California (Mediterranean climate), and Japan (humid continental climate; Stock and Montgomery, 1999), as well as the Siwalik Hills in Himalaya (monsoon highland climate; Kirby and Whipple, 2001), and the Ukak River in Alaska (cool continental climate; Whipple et al., 2000b).

355 It is difficult to isolate the influence of rock strength from climate conditions in this comparison. Nonetheless, Fig. 7 suggests a stark contrast over orders of magnitude in the fluvial erosion efficiency coefficient between tectonically active and inactive settings, which may result from the disparity between the high rates of denudation in orogenic belts, with exposure of mineral surfaces that are readily weathered, and the long timescales of evolution in ancient mountain belts, where the hard metamorphic roots of these landscapes are progressively exhumed as these landscapes age ~~they get older~~ (Summerfield and Hulton, 1994;
360 Bishop, 2007; Braun et al., 2014; Bursztyn et al., 2015). In contrast, the global dataset of stream-power model parameters reported by Harel et al. (2016) exhibits lower K values in tectonically active areas compared to higher K values in inactive settings. These authors concluded that such results were counter-intuitive and highlighted the fact that K is not well calibrated (Harel et al., 2016); more work needs to be dedicated to the determination of K and what controls its variations.

5.3 Landscape development in a decaying mountain belt marked by lateral contrasts in rock strength

365 Our findings indicate that high-relief uplands underlain by resistant bedrock are denuding more slowly than lower-relief surrounding areas associated with more erodible lithologies, with the corollary that topographic relief must still be growing instead of decaying in this tectonically quiescent landscape. ~~Persistence of these denudation rates (averaged over timescales up to 1.1 Myr; Table S1) implies that relief in this ancient orogen is still growing rather than decaying. In this situation, relief grows not only because of the unequal denudation pattern across the landscape but also as a result of the flexural-isostatic~~
370 ~~compensation~~ Furthermore, the expected isostatic compensation to ~~the~~ denudational unloading (e.g., Bishop and Brown, 1992), which is a process that occurs at a much ~~wider~~ longer wavelength than the local changes in lithology and denudation rates (Gilchrist and Summerfield, 1990; Watts et al. 2000), implies that uplands and surrounding areas are equally isostatically uplifted in response to the regional denudation, likely resulting in a net reduction of mean elevation over time, but a slight

increase in the heights of mountain peaks, ~~similar to~~ as has been proposed by Molnar and England (1990). The timescale over which relief might continue to grow simply as a result of spatial variations in bedrock lithology is unresolved. However, our results suggest that relief is likely to persist long into the future in a landscape that would otherwise be suited to rapid denudation (high-relief, and relatively high precipitation rates and warm climate).

Extrapolation ~~The extrapolated effect~~ of the denudation pattern in the QF over time, which is speculative for timescales more extended than the averaging of our cosmogenic data (Table S1), ~~simplistic as it considers that geology does not vary with depth over the long timescales of post-orogenic evolution, does not~~ suggests ~~that topographic rejuvenation has not affected the study area, but instead~~ that ~~the exposition~~ exposure at the surface of rocks with significant contrasts in erodibility naturally favours the survival of relief in the absence of ongoing tectonics. ~~On the contrary~~ Nevertheless, we have compelling geomorphic evidence that at least some decaying mountain belts underwent spatial and temporal changes in denudation rates as a response to different types of forcing (e.g., tectonic, lithologic, climatic, mantle-driven, and far-field driven) long after cessation of crustal thickening (e.g., Pazzaglia and Brandon, 1996; Quigley et al., 2007; Gallen et al., 2013; Tucker and van der Beek, 2013; Liu, 2014; Gallen, 2018). In this situation, large spatial contrasts in the fluvial erosion efficiency coefficient (K), such as ~~the~~ observed in our study area, determine significant differences in erosional response times across the landscape (i.e., the timescale of channel profile response to perturbations in boundary conditions), with response times (T_d) decreasing as K increases (T_d scales to $1/K^n$, where n is the slope exponent in the stream-power model; Baldwin et al., 2013). ~~and thus~~ Spatial gradients in K thus ~~controls~~ how post-orogenic landscapes respond to a driving force. Indeed, lithological controls on post-orogenic landscape dynamics have long been identified (e.g., Hack, 1960, 1975; Twidale, 1976; Mills, 2003; Bishop and Goldrick, 2010; Spotila et al., 2015; Gallen, 2018; Bernard et al., 2019; Vasconcelos et al., 2019; Zondervan et al., 2020a). ~~and,~~ Nonetheless, lithological contrasts have not been addressed adequately by numerical modelling of post-orogenic landscape evolution and, in particular, topographic decay (e.g., Baldwin et al., 2003; Egholm et al., 2013).

395 6 Conclusion

We present ^{10}Be concentrations in river sand from catchments spanning the range in topographic metrics and bedrock erodibility in a humid ~~semitropical~~ subtropical, tectonically inactive landscape in Brazil. The results of this study suggest that the post-orogenic history of the study area is not a progressive reduction in relief and denudation rates. Instead, the exposure ~~at the surface of rocks with strong lateral contrasts in erodibility amplifies spatial differences in topographic forms and denudation rates over time,~~ ~~which sustains~~ or, indeed, increases relief in a tectonically dead landscape. ~~We show that~~ Spatial variations in topographic relief and channel steepness ~~can be~~ are explained by changes in rock type in the study area, and yet denudation rates are not ~~uniformly distributed~~ spatially uniform. ~~Given the long period since the cessation of crustal thickening, we conjecture~~ Contrasts in rock type continue to drive differences in denudation rates in a decaying mountain belt evolving over the Myr timescale, indicating that the landscape has not achieved equilibrium. ~~and that equilibrium is not a natural attractor in ancient landscapes. Our results indicate that the fluvial erosion efficiency differs by three orders of~~

~~magnitude in the study area, varying as a function of rock type.~~ This study demonstrates that lateral variations in rock strength play an essential role in the dynamics of an ancient mountain belt, and likely in other post-orogenic settings characterised by ~~lithological~~ spatial heterogeneity in lithology. Such lithological heterogeneity, ~~in which they~~ controls the tempo and style of landscape response to changes in boundary conditions while also affecting the ~~ir~~ pattern of landscape denudation.

410 7 Data availability

The data supporting the findings of this study are available in the Supplemental Material, including ^{10}Be analytical results and derived denudation rate data, catchment-averaged geomorphic parameters, and detailed information on catchment lithology. Extraction of topographic metrics and catchment-averaged pressure were carried out using LSDTopoTools version 2.03 (Mudd et al., 2020).

415 8 Author contributions

D.P. designed the study with contributions from all co-authors. D.P. and D.F. performed the cosmogenic isotope analysis. D.P. quantified the geomorphic parameters. D.P., C.P., M.D.H, P.B., and D.F. wrote the manuscript. D.P produced the Figures.

9 Competing interests

The authors declare no competing interests.

420 10 Acknowledgements

We thank the German Aerospace Center (DLR), the Natural Environment Research Council (NERC), and the Coordination for the Improvement of Higher Education Personnel (CAPES) for research support. We thank Hugh D. Sinclair for providing feedback on an early version of the manuscript.

11 Financial support

425 The DLR granted us access to TanDEM-X data as part of the project DEM_GEOL1345. NERC supported the cosmogenic isotope analysis under the CIAF award number 9177.0417. D.P. had support from CAPES under a Science without Borders fellowship (n° BEX 12000/13-2) and, subsequently, a CAPES-PrInt Postdoctoral fellowship (n° 88887.367976 / 2019-00).

12 References

- Ahnert, F.: Functional relationships between denudation, relief, and uplift in large, mid-latitude drainage basins, *Am. J. Sci.*, 268, 243–263, <https://doi.org/10.2475/ajs.268.3.243>, 1970.
- Alkmim, F.F. and Marshak, S.: Transamazonian orogeny in the Southern Sao Francisco craton region, Minas Gerais, Brazil: evidence for Paleoproterozoic collision and collapse in the Quadrilátero Ferrífero, *Precambrian Res.*, 90, 29–58, [https://doi.org/10.1016/S0301-9268\(98\)00032-1](https://doi.org/10.1016/S0301-9268(98)00032-1), 1998.
- [Alvares, C.A., Stape, J.L., Sentelhas, P.C., de Moraes Gonçalves, J.L. and Sparovek, G.: Köppen's climate classification map for Brazil, *Meteorol. Z.*, 22, 711–728, <https://doi.org/10.1127/0941-2948/2013/0507>, 2013.](#)
- Balco, G., Stone, J.O., Lifton, N.A. and Dunai, T.J.: A complete and easily accessible means of calculating surface exposure ages or erosion rates from ^{10}Be and ^{26}Al measurements, *Quat. Geochronol.*, 3, 174–195, <https://doi.org/10.1016/j.quageo.2007.12.001>, 2008.
- Baldwin, J.A., Whipple, K.X. and Tucker, G.E.: Implications of the shear stress river incision model for the timescale of postorogenic decay of topography, *J. Geophys. Res.-Sol. Ea.*, 108, 7(1)–7(17), <https://doi.org/10.1029/2001JB000550>, 2003.
- Barreto, H.N., Varajão, C.A., Braucher, R., Bourlès, D.L., Salgado, A.A. and Varajão, A.F.: Denudation rates of the Southern Espinhaço Range, Minas Gerais, Brazil, determined by in situ-produced cosmogenic beryllium-10, *Geomorphology*, 191, 1–13, <https://doi.org/10.1016/j.geomorph.2013.01.021>, 2013.
- Beeson, H.W., McCoy, S.W. and Keen-Zebert, A.: Geometric disequilibrium of river basins produces long-lived transient landscapes, *Earth Planet. Sc. Lett.*, 475, 34–43, <https://doi.org/10.1016/j.epsl.2017.07.010>, 2017.
- Bernard, T., Sinclair, H.D., Gailleton, B., Mudd, S.M. and Ford, M.: Lithological control on the post-orogenic topography and erosion history of the Pyrenees, *Earth Planet. Sc. Lett.*, 518, 53–66, <https://doi.org/10.1016/j.epsl.2019.04.034>, 2019.
- Bierman, P.R. and Caffee, M.: Slow rates of rock surface erosion and sediment production across the Namib Desert and escarpment, southern Africa, *Am. J. Sci.*, 301, 326–358, <https://doi.org/10.2475/ajs.301.4-5.326>, 2001.
- Bishop, P.: Long-term landscape evolution: linking tectonics and surface processes, *Earth Surf. Proc. Land.*, 32, 329–365, <https://doi.org/10.1002/esp.1493>, 2007.
- Bishop, P. and Brown, R.: Denudational isostatic rebound of intraplate highlands: the Lachlan River valley, Australia, *Earth Surf. Proc. Land.*, 17, 345–360, <https://doi.org/10.1002/esp.3290170405>, 1992.
- Bishop, P. and Goldrick, G.: Lithology and the evolution of bedrock rivers in post-orogenic settings: constraints from the high-elevation passive continental margin of SE Australia, *Geol. Soc. Spec. Publ.*, 346, 267–287, <https://doi.org/10.1144/SP346.14>, 2010.

- Blackburn, T., Ferrier, K.L. and Perron, J.T.: Coupled feedbacks between mountain erosion rate, elevation, crustal temperature, and density, *Earth Planet. Sc. Lett.*, 498, 377–386, <https://doi.org/10.1016/j.epsl.2018.07.003>, 2018.
- Braun, J., Simon-Labric, T., Murray, K.E. and Reiners, P.W.: Topographic relief driven by variations in surface rock
460 density, *Nat. Geosci.*, 7, 534–540, <https://doi.org/10.1038/NGEO2171>, 2014.
- Bursztyn, N., Pederson, J.L., Tressler, C., Mackley, R.D. and Mitchell, K.J.: Rock strength along a fluvial transect of the Colorado Plateau—quantifying a fundamental control on geomorphology, *Earth Planet. Sc. Lett.*, 429, 90–100, <https://doi.org/10.1016/j.epsl.2015.07.042>, 2015.
- Campforts, B., Vanacker, V., Herman, F., Vanmaercke, M., Schwanghart, W., Tenorio, G.E., Willems, P. and Govers, G.:
465 Parameterisation of river incision models requires accounting for environmental heterogeneity: insights from the tropical Andes, *Earth Surf. Dynam.*, 8, 447–447, <https://doi.org/10.5194/esurf-8-447-2020>, 2020.
- Chemale Jr, F., Rosière, C.A. and Endo, I.: The tectonic evolution of the Quadrilátero Ferrífero, Minas Gerais, Brazil, *Precambrian Res.*, 65, 25–54, [https://doi.org/10.1016/0301-9268\(94\)90098-1](https://doi.org/10.1016/0301-9268(94)90098-1), 1994.
- Clubb, F.J., Bookhagen, B. and Rheinwalt, A.: Clustering river profiles to classify geomorphic domains, *J. Geophys. Res.-*
470 *Earth*, 124, 1417–1439, <https://doi.org/10.1029/2019JF005025>, 2019.
- Cyr, A.J., Granger, D.E., Olivetti, V. and Molin, P.: Distinguishing between tectonic and lithologic controls on bedrock channel longitudinal profiles using cosmogenic ^{10}Be erosion rates and channel steepness index, *Geomorphology*, 209, 27–38, <https://doi.org/10.1016/j.geomorph.2013.12.010>, 2014.
- Davis, W.M.: The geographical cycle, *Geogr. J.*, 14, 481–504, <https://doi.org/10.2307/1774538>, 1899.
- DiBiase, R.A.: Increasing vertical attenuation length of cosmogenic nuclide production on steep slopes negates topographic
475 shielding corrections for catchment erosion rates, *Earth Surf. Dynam.*, 6, 923–931, <https://doi.org/10.5194/esurf-6-923-2018>, 2018.
- DiBiase, R.A. and Whipple, K.X.: The influence of erosion thresholds and runoff variability on the relationships among topography, climate, and erosion rate, *J. Geophys. Res.-Earth*, 116, 1–17, <https://doi.org/10.1029/2011JF002095>, 2011.
- DiBiase, R.A., Whipple, K.X., Heimsath, A.M. and Ouimet, W.B.: Landscape form and millennial erosion rates in the San
480 Gabriel Mountains, CA, *Earth Planet. Sc. Lett.*, 289, 134–144, <https://doi.org/10.1016/j.epsl.2009.10.036>, 2010.
- Dorr, J.V.N.: Physiographic, stratigraphic, and structural development of the Quadrilátero Ferrífero, Minas Gerais, Brazil, United States Geological Survey Professional Paper 641-A, US Geological Survey, Washington, D.C., 1969.
- Duvall, A., Kirby, E. and Burbank, D.: Tectonic and lithologic controls on bedrock channel profiles and processes in coastal
485 California, *J. Geophys. Res.-Earth*, 109, 1–18, <https://doi.org/10.1029/2003JF000086>, 2004.

- Egholm, D.L., Knudsen, M.F. and Sandiford, M.: Lifespan of mountain ranges scaled by feedbacks between landsliding and erosion by rivers, *Nature*, 498, 475–478, <https://doi.org/10.1038/nature12218>, 2013.
- Ferrier, K.L., Huppert, K.L. and Perron, J.T.: Climatic control of bedrock river incision, *Nature*, 496, 206–209, <https://doi.org/10.1038/nature11982>, 2013.
- 490 Fick, S.E. and Hijmans, R.J.: WorldClim 2: new 1-km spatial resolution climate surfaces for global land areas, *Int. J. Climatol.*, 37, 4302–4315, <https://doi.org/10.1002/joc.5086>, 2017.
- Flint, J.J.: Stream gradient as a function of order, magnitude, and discharge, *Water Resour. Res.*, 10, 969–973, <https://doi.org/10.1029/WR010i005p00969>, 1974.
- Forte, A.M., Yanites, B.J. and Whipple, K.X.: Complexities of landscape evolution during incision through layered
495 stratigraphy with contrasts in rock strength, *Earth Surf. Proc. Land.*, 41, 1736–1757, <https://doi.org/10.1002/esp.3947>, 2016.
- Gallen, S.F.: Lithologic controls on landscape dynamics and aquatic species evolution in post-orogenic mountains, *Earth Planet. Sc. Lett.*, 493, 150–160, <https://doi.org/10.1016/j.epsl.2018.04.029>, 2018.
- Gallen, S.F., Wegmann, K.W. and Bohnenstiehl, D.R.: Miocene rejuvenation of topographic relief in the southern Appalachians, *GSA Today*, 23, 4–10, <https://doi.org/10.1130/GSATG163A.1>, 2013.
- 500 Gilbert, G.: *Geology of the Henry Mountains*, USGS Unnumbered Series, Government Printing Office, Washington, D.C., USA, <https://doi.org/10.3133/70038096>, 1877.
- Gilchrist, A.R. and Summerfield, M.A.: Differential denudation and flexural isostasy in formation of rifted-margin upwarps, *Nature*, 346, 739–742, <https://doi.org/10.1038/346739a0>, 1990.
- Hack, J.T.: Interpretation of erosional topography in humid temperate regions, *Am. J. Sci.*, 258, 80–97, 1960.
- 505 Hack, J.T.: Dynamic equilibrium and landscape evolution, in: *Theories of landform development*, edited by: Melhorn, W.N., and Flemal, R.C., State University of New York Press, Binghamton, NY, USA, 87–102, 1975.
- Hack, J.T.: *Physiographic divisions and differential uplift in the Piedmont and Blue Ridge*, United States Geological Survey Professional Paper 1265, US Geological Survey, Washington, D.C., 1982.
- Harel, M.A., Mudd, S.M. and Attal, M.: Global analysis of the stream power law parameters based on worldwide ¹⁰Be
510 denudation rates, *Geomorphology*, 268, 184–196, <https://doi.org/10.1016/j.geomorph.2016.05.035>, 2016.
- Hergarten, S., Robl, J. and Stüwe, K.: Tectonic geomorphology at small catchment sizes-extensions of the stream-power approach and the χ method, *Earth Surf. Dynam.*, 4, 1–9, <https://doi.org/10.5194/esurf-4-1-2016>, 2016.
- Howard, A.D. and Kerby, G.: Channel changes in badlands, *GSA Bulletin*, 94, 739–752, [https://doi.org/10.1130/0016-7606\(1983\)94<739:CCIB>2.0.CO;2](https://doi.org/10.1130/0016-7606(1983)94<739:CCIB>2.0.CO;2), 1983.

- 515 Hurst, M.D., Ellis, M.A., Royse, K.R., Lee, K.A. and Freeborough, K.: Controls on the magnitude-frequency scaling of an inventory of secular landslides, *Earth Surf. Dynam.*, 1, 67–78, <https://doi.org/10.5194/esurf-1-67-2013>, 2013.
- Jansen, J.D., Codilean, A.T., Bishop, P. and Hoey, T.B.: Scale dependence of lithological control on topography: Bedrock channel geometry and catchment morphometry in western Scotland, *J. Geol.*, 118, 223–246, <https://doi.org/10.1086/651273>, 2010.
- 520 Kirby, E. and Whipple, K.X.: Quantifying differential rock-uplift rates via stream profile analysis, *Geology*, 29, 415–418. [https://doi.org/10.1130/0091-7613\(2001\)029<0415:QDRURV>2.0.CO;2](https://doi.org/10.1130/0091-7613(2001)029<0415:QDRURV>2.0.CO;2), 2001.
- Kirby, E. and Whipple, K.X.: Expression of active tectonics in erosional landscapes, *J. Struct. Geol.*, 44, 54–75, <https://doi.org/10.1016/j.jsg.2012.07.009>, 2012.
- Kohl, C.P. and Nishiizumi, K.: Chemical isolation of quartz for measurement of *in-situ*-produced cosmogenic
- 525 nuclides, *Geochim. Cosmochim. Ac.*, 56, 3583–3587, [https://doi.org/10.1016/0016-7037\(92\)90401-4](https://doi.org/10.1016/0016-7037(92)90401-4), 1992.
- Korup, O.: Rock type leaves topographic signature in landslide-dominated mountain ranges, *Geophys. Res. Lett.*, 35, 1–5, <https://doi.org/10.1029/2008GL034157>, 2008.
- Lague, D.: The stream power river incision model: evidence, theory and beyond, *Earth Surf. Proc. Land.*, 39, 38–61, <https://doi.org/10.1002/esp.3462>, 2014.
- 530 Lague, D., Davy, P. and Crave, A.: Estimating uplift rate and erodibility from the area-slope relationship: Examples from Brittany (France) and numerical modelling, *Phys. Chem. Earth, Part A*, 25, 543–548, [https://doi.org/10.1016/S1464-1895\(00\)00083-1](https://doi.org/10.1016/S1464-1895(00)00083-1), 2000.
- Lal, D.: Cosmic ray labeling of erosion surfaces: in situ nuclide production, *Earth Planet. Sc. Lett.*, 104, 424–439. [https://doi.org/10.1016/0012-821X\(91\)90220-C](https://doi.org/10.1016/0012-821X(91)90220-C), 1991.
- 535 Liu, L.: Rejuvenation of Appalachian topography caused by subsidence-induced differential erosion, *Nat. Geosci.*, 7, 518–523, <https://doi.org/10.1038/NGEO2187>, 2014.
- Lobato, L.M.; Baltazar, O.F.; Reis, L.B.; Achtschin, A.B.; Baars, F.J.; Timbó, M.A.; Berni, G.V; Mendonça, B.R.V. de; and Ferreira, D.V: Projeto Geologia do Quadrilátero Ferrífero - Integração e Correção Cartográfica em SIG com Nota Explicativa, CODEMIG, Belo Horizonte, 2005.
- 540 Lobato, L., Ribeiro-Rodrigues, L., Zucchetti, M., Noce, C., Baltazar, O., Da Silva, L. and Pinto, C.: Brazil's premier gold province. Part I: The tectonic, magmatic, and structural setting of the Archean Rio das Velhas greenstone belt, Quadrilátero Ferrífero, *Miner. Deposita.*, 36, 228–248. <https://doi.org/10.1007/s001260100179>, 2001.

- Mandal, S.K., Lupker, M., Burg, J.P., Valla, P.G., Haghipour, N. and Christl, M.: Spatial variability of ^{10}Be -derived erosion rates across the southern Peninsular Indian escarpment: A key to landscape evolution across passive margins, *Earth Planet. Sc. Lett.*, 425, 154–167, <https://doi.org/10.1016/j.epsl.2015.05.050>, 2015.
- Matmon, A., Bierman, P.R., Larsen, J., Southworth, S., Pavich, M. and Caffee, M.: Temporally and spatially uniform rates of erosion in the southern Appalachian Great Smoky Mountains, *Geology*, 31, 155–158, [https://doi.org/10.1130/0091-7613\(2003\)031<0155:TASURO>2.0.CO;2](https://doi.org/10.1130/0091-7613(2003)031<0155:TASURO>2.0.CO;2), 2003.
- Meybeck, M.: Global chemical weathering of surficial rocks estimated from river dissolved loads, *Am. J. Sci.*, 287, 401–428, <https://doi.org/10.2475/ajs.287.5.401>, 1987.
- Miller, S.R., Sak, P.B., Kirby, E. and Bierman, P.R.: Neogene rejuvenation of central Appalachian topography: Evidence for differential rock uplift from stream profiles and erosion rates, *Earth Planet. Sc. Lett.*, 369, 1–12, <https://doi.org/10.1016/j.epsl.2013.04.007>, 2013.
- Mills, H.H.: Inferring erosional resistance of bedrock units in the east Tennessee mountains from digital elevation data, *Geomorphology*, 55, 263–281, [https://doi.org/10.1016/S0169-555X\(03\)00144-2](https://doi.org/10.1016/S0169-555X(03)00144-2), 2003.
- Molnar, P. and England, P.: Late Cenozoic uplift of mountain ranges and global climate change: chicken or egg?, *Nature*, 346, 29–34, <https://doi.org/10.1038/346029a0>, 1990.
- [Monteiro, H.S., Vasconcelos, P.M., Farley, K.A., Spier, C.A. and Mello, C.L.: \(U–Th\)/He geochronology of goethite and the origin and evolution of cangas, *Geochim. Cosmochim. Ac.*, 131, 267–289, <https://doi.org/10.1016/j.gca.2014.01.036>, 2014.](#)
- Monteiro, H.S., Vasconcelos, P.M. and Farley, K.A.: A combined (U-Th)/He and cosmogenic ^3He record of landscape armoring by biogeochemical iron cycling, *J. Geophys. Res.-Earth*, 123, 298–323, <https://doi.org/10.1002/2017JF004282>, 2018.
- Montgomery, D.R.: Slope distributions, threshold hillslopes, and steady-state topography, *Am. J. Sci.*, 301, 432–454, <https://doi.org/10.2475/ajs.301.4-5.432>, 2001.
- Montgomery, D.R. and Brandon, M.T.: Topographic controls on erosion rates in tectonically active mountain ranges, *Earth Planet. Sc. Lett.*, 201, 481–489, [https://doi.org/10.1016/S0012-821X\(02\)00725-2](https://doi.org/10.1016/S0012-821X(02)00725-2), 2002.
- Moon, S., Chamberlain, C.P., Blisniuk, K., Levine, N., Rood, D.H. and Hilley, G.E.: Climatic control of denudation in the deglaciated landscape of the Washington Cascades, *Nat. Geosci.*, 4, 469–473, <https://doi.org/10.1038/NGEO1159>, 2011.
- Mudd, S.M., Attal, M., Milodowski, D.T., Grieve, S.W. and Valters, D.A.: A statistical framework to quantify spatial variation in channel gradients using the integral method of channel profile analysis, *J. Geophys. Res.-Earth*, 119, 138–152, <https://doi.org/10.1002/2013JF002981>, 2014.

- Mudd, S.M., Harel, M.A., Hurst, M.D., Grieve, S.W. and Marrero, S.M.: The CAIRN method: automated, reproducible calculation of catchment-averaged denudation rates from cosmogenic nuclide concentrations, *Earth Surf. Dynam.*, 4, 655–674, <https://doi.org/10.5194/esurf-4-655-2016>, 2016.
- 575 Mudd, S.M., Clubb, F.J., Gailleton, B. and Hurst, M.D.: How concave are river channels?, *Earth Surf. Dynam.*, 6, 505–523, <https://doi.org/10.5194/esurf-6-505-2018>, 2018.
- Mudd, S. M., Clubb, F. J., Hurst, M. D.: LSDTopoTools2 v0.3, Zenodo, <https://doi.org/10.5281/zenodo.3769703>, 2020.
- Myers, R.H. (2nd Edition): *Classical and modern regression with applications*, Duxbury Press, Boston, MA, USA, 1990.
- Pazzaglia, F.J. and Brandon, M.T.: Macrogeomorphic evolution of the post-Triassic Appalachian mountains determined by
 580 deconvolution of the offshore basin sedimentary record, *Basin Res.*, 8, 255–278, <https://doi.org/10.1046/j.1365-2117.1996.00274.x>, 1996.
- Perne, M., Covington, M.D., Thaler, E.A. and Myre, J.M.: Steady state, erosional continuity, and the topography of landscapes developed in layered rocks, *Earth Surf. Dynam.*, 5, 85–100, <https://doi.org/10.5194/esurf-5-85-2017>, 2017.
- Perron, J.T. and Royden, L.: An integral approach to bedrock river profile analysis, *Earth Surf. Proc. Land.*, 38, 570–576,
 585 <https://doi.org/10.1002/esp.3302>, 2013.
- Portenga, E.W. and Bierman, P.R.: Understanding Earth's eroding surface with ¹⁰Be, *GSA Today*, 21, 4–10, <https://doi.org/10.1130/G111A.1>, 2011.
- Quigley, M., Sandiford, M., Fifield, K. and Alimanovic, A.: Bedrock erosion and relief production in the northern Flinders Ranges, Australia, *Earth Surf. Proc. Land.*, 32, 929–944, <https://doi.org/10.1002/esp.1459>, 2007.
- 590 Roberts, G.G. and White, N.: Estimating uplift rate histories from river profiles using African examples, *J. Geophys. Res.-Earth*, 115, 1–24, <https://doi.org/10.1029/2009JB006692>, 2010.
- Salgado, A.A.R., Braucher, R., Varajão, A.C., Colin, F., Varajão, A.F.D.C. and Nalini Jr, H.A.: Relief evolution of the Quadrilátero Ferrífero (Minas Gerais, Brazil) by means of (¹⁰Be) cosmogenic nuclei, *Z. Geomorphol.*, 52, 317–323, <https://doi.org/10.1127/0372-8854/2008/0052-0317>, 2008.
- 595 Sant'Anna, L.G., Schorscher, H.D. and Riccomini, C.: Cenozoic tectonics of the Fonseca basin region, eastern Quadrilátero Ferrífero, MG, Brazil, *J. S. Am. Earth Sci.*, 10, 275–284, [https://doi.org/10.1016/S0895-9811\(97\)00016-3](https://doi.org/10.1016/S0895-9811(97)00016-3), 1997.
- Scharf, T.E., Codilean, A.T., De Wit, M., Jansen, J.D. and Kubik, P.W.: Strong rocks sustain ancient postorogenic topography in southern Africa, *Geology*, 41, 331–334, <https://doi.org/10.1130/G33806.1>, 2013.

- Snyder, N.P., Whipple, K.X., Tucker, G.E. and Merritts, D.J.: Landscape response to tectonic forcing: Digital elevation model analysis of stream profiles in the Mendocino triple junction region, northern California, GSA Bulletin, 112, 1250–1263, [https://doi.org/10.1130/0016-7606\(2000\)112<1250:LRTTFD>2.0.CO;2](https://doi.org/10.1130/0016-7606(2000)112<1250:LRTTFD>2.0.CO;2), 2000.
- [Spier, C.A., Vasconcelos, P.M. and Oliviera, S.M.: \$^{40}\text{Ar}/^{39}\text{Ar}\$ geochronological constraints on the evolution of lateritic iron deposits in the Quadrilátero Ferrífero, Minas Gerais, Brazil, Chem. Geol., 234, 79–104, <https://doi.org/10.1016/j.chemgeo.2006.04.006>, 2006.](https://doi.org/10.1016/j.chemgeo.2006.04.006)
- Spotila, J.A., Moskey, K.A. and Prince, P.S.: Geologic controls on bedrock channel width in large, slowly-eroding catchments: Case study of the New River in eastern North America, Geomorphology, 230, 51–63, <https://doi.org/10.1016/j.geomorph.2014.11.004>, 2015.
- Stock, J.D. and Montgomery, D.R.: Geologic constraints on bedrock river incision using the stream power law, J. Geophys. Res.-Sol. Ea., 104, 4983–4993, <https://doi.org/10.1029/98JB02139>, 1999.
- Stone, J.O.: Air pressure and cosmogenic isotope production, J. Geophys. Res.-Sol. Ea., 105, 23753–23759, <https://doi.org/10.1029/2000JB900181>, 2000.
- Strahler, A.N.: Quantitative analysis of watershed geomorphology, Eos, 38, 913–920, <https://doi.org/10.1029/TR038i006p00913>, 1957.
- Summerfield, M.A. and Hulton, N.J.: Natural controls of fluvial denudation rates in major world drainage basins, J. Geophys. Res.-Sol. Ea., 99, 13871–13883, <https://doi.org/10.1029/94JB00715>, 1994.
- Tucker, G.E. and van Der Beek, P.: A model for post-orogenic development of a mountain range and its foreland, Basin Res., 25, 241–259, <https://doi.org/10.1111/j.1365-2117.2012.00559.x>, 2013.
- Twidale, C.R.: On the survival of paleoforms, Am. J. Sci., 276, 77–95, <https://doi.org/10.2475/ajs.276.1.77>, 1976.
- Vasconcelos, P.M. and Carmo, I.D.O.: Calibrating denudation chronology through $^{40}\text{Ar}/^{39}\text{Ar}$ weathering geochronology, Earth-Sci. Rev., 179, 411–435, <https://doi.org/10.1016/j.earscirev.2018.01.003>, 2018.
- Vasconcelos, P.M., Farley, K.A., Stone, J., Piacentini, T. and Fifield, L.K.: Stranded landscapes in the humid tropics: Earth's oldest land surfaces, Earth Planet. Sc. Lett., 519, 152–164, <https://doi.org/10.1016/j.epsl.2019.04.014>, 2019.
- von Blanckenburg, F., Hewawasam, T. and Kubik, P.W.: Cosmogenic nuclide evidence for low weathering and denudation in the wet, tropical highlands of Sri Lanka, J. Geophys. Res.-Earth, 109, 1–22, <https://doi.org/10.1029/2003JF000049>, 2004.
- [Watts, A.B., McKerrow, W.S. and Fielding, E.: Lithospheric flexure, uplift, and landscape evolution in south-central England, J. Geol. Soc., 157, 1169–1177, <https://doi.org/10.1144/jgs.157.6.1169>, 2000.](https://doi.org/10.1144/jgs.157.6.1169)

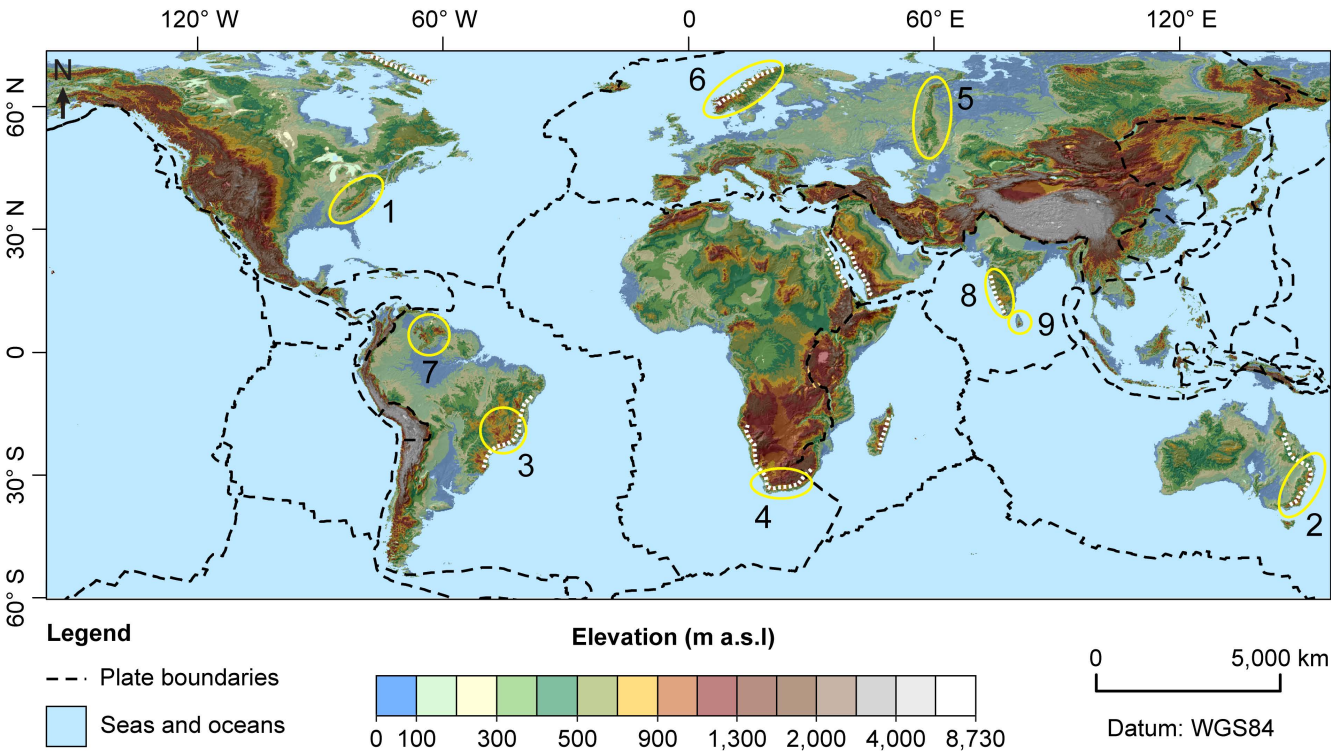
- Whipple, K.X. and Tucker, G.E.: Dynamics of the stream-power river incision model: Implications for height limits of mountain ranges, landscape response timescales, and research needs, *J. Geophys. Res.-Sol. Ea.*, 104, 17661–17674, <https://doi.org/10.1029/1999JB900120>, 1999.
- 630 Whipple, K.X., Hancock, G.S. and Anderson, R.S.: River incision into bedrock: Mechanics and relative efficacy of plucking, abrasion, and cavitation, *GSA Bulletin*, 112, 490–503, [https://doi.org/10.1130/0016-7606\(2000\)112<490:RIIBMA>2.0.CO;2](https://doi.org/10.1130/0016-7606(2000)112<490:RIIBMA>2.0.CO;2), 2000a.
- Whipple, K.X., Snyder, N.P. and Dollenmayer, K.: Rates and processes of bedrock incision by the Upper Ukak River since the 1912 Novarupta ash flow in the Valley of Ten Thousand Smokes, Alaska, *Geology*, 28, 835–838, 635 [https://doi.org/10.1130/0091-7613\(2000\)28<835:RAPOBI>2.0.CO;2](https://doi.org/10.1130/0091-7613(2000)28<835:RAPOBI>2.0.CO;2), 2000b.
- White, A.F. and Blum, A.E.: Effects of climate on chemical weathering in watersheds, *Geochim. Cosmochim. Ac.*, 59, 1729–1747, [https://doi.org/10.1016/0016-7037\(95\)00078-E](https://doi.org/10.1016/0016-7037(95)00078-E), 1995.
- [Zondervan, J.R., Stokes, M., Boulton, S.J., Telfer, M.W. and Mather, A.E.: Rock strength and structural controls on fluvial erodibility: Implications for drainage divide mobility in a collisional mountain belt, *Earth Planet. Sc. Lett.*, 538, 1–13, <https://doi.org/10.1016/j.epsl.2020.116221>, 2020a.](https://doi.org/10.1016/j.epsl.2020.116221)
- 640 <https://doi.org/10.1016/j.epsl.2020.116221>, 2020a.
- Zondervan, J.R., Whittaker, A.C., Bell, R.E., Watkins, S.E., Brooke, S.A. and Hann, M.G: New constraints on bedrock erodibility and landscape response times upstream of an active fault, *Geomorphology*, 351, 1–14, <https://doi.org/10.1016/j.geomorph.2019.106937>, [2020b](#).

13 Tables

645 **Table 1: Variability in θ in the QF.** Best-fit θ values were computed for all catchments of stream-order higher than third-order based on the disorder method (Hergarten et al., 2016) using code developed by Mudd et al. (2018).

Stream-order	Number of basins	Best-fit θ statistics	
		Mean θ	Standard deviation
fourth-order	114	0.37	0.17
fifth-order	24	0.45	0.12
sixth-order	5	0.46	0.08
seventh-order	1	0.53	-
all catchments	144	0.44	0.13

14 Figures



650 **Figure 1: Global elevation and striking examples of high-relief ancient mountain belts.** Post-orogenic settings highlighted by yellow ellipses: (1) the Appalachian Mountains; (2) SE Australia; (3) SE Brazil; (4) the Cape Mountains; (5) the Ural Mountains; (6) the Scandinavian Caledonides; (7) the Guyana Shield; (8) the Western Ghats; and (9) the Sri Lanka orogen. White dotted lines represent high-elevation passive margins. We extracted elevation data from the U.S. Geological Survey's (USGS) Global Multi-resolution Terrain Elevation data 2010 (GMTED2010).

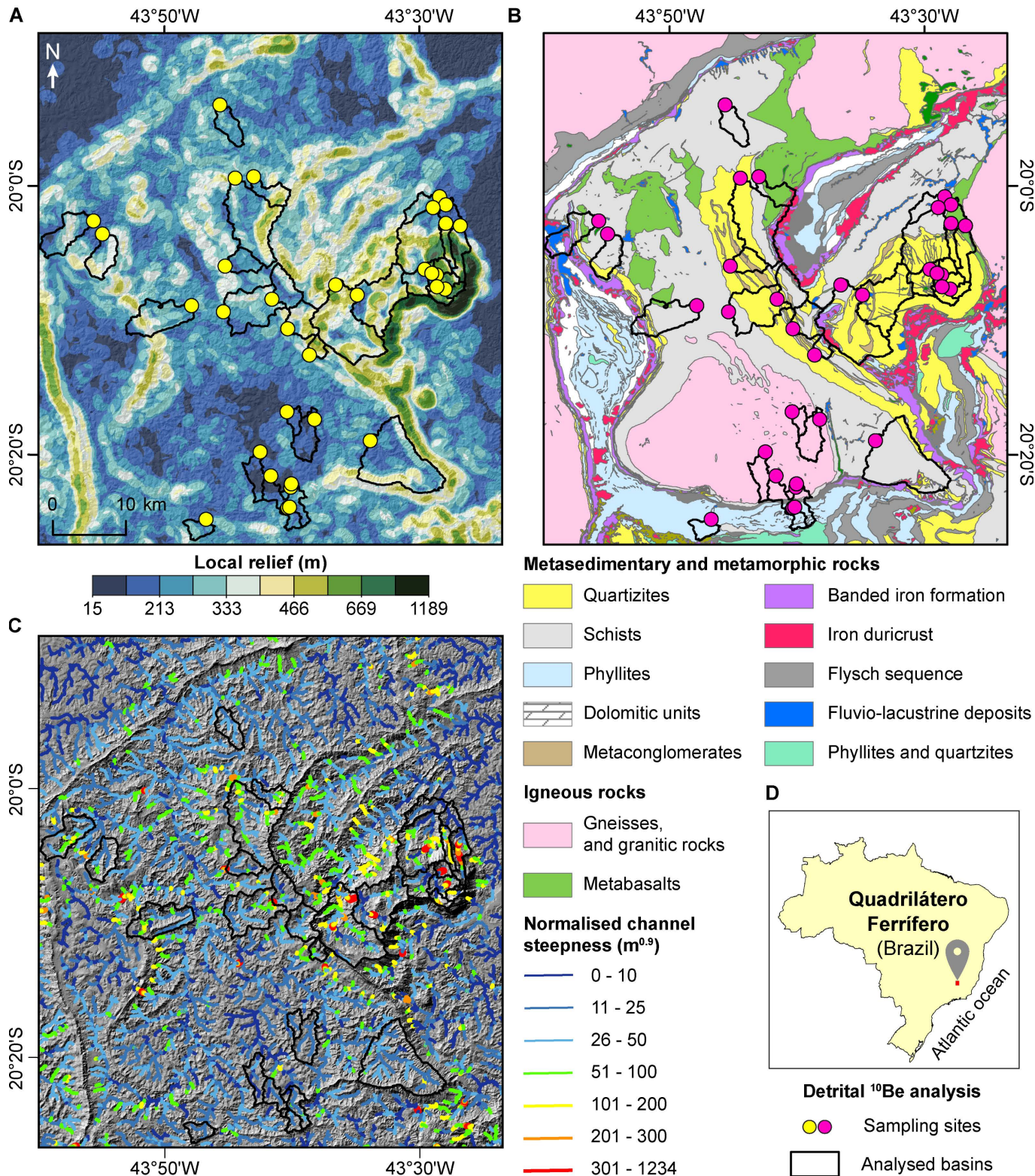


Figure 2: The geomorphic context of the Quadrilátero Ferrífero – Brazil. (A) Map of local topographic relief (extracted using a 2-km diameter window). (B) Simplified bedrock geology in the study area, comprising mostly steeply dipping ($\geq 35^\circ$), Archean and Paleoproterozoic sequences. (C) Map of normalised channel steepness (k_{sn}) extracted using the segmentation method of Mudd et al., (2014), with θ_{ref} of 0.45. Note that we used an area threshold of 1.0 km^2 to extract the drainage network, and we did not show sampling sites in panel (C) for illustration purposes. (D) The location of the QF in Brazil, $\sim 340 \sim 350 \text{ km}$ away (in a straight line) from the Atlantic Ocean.

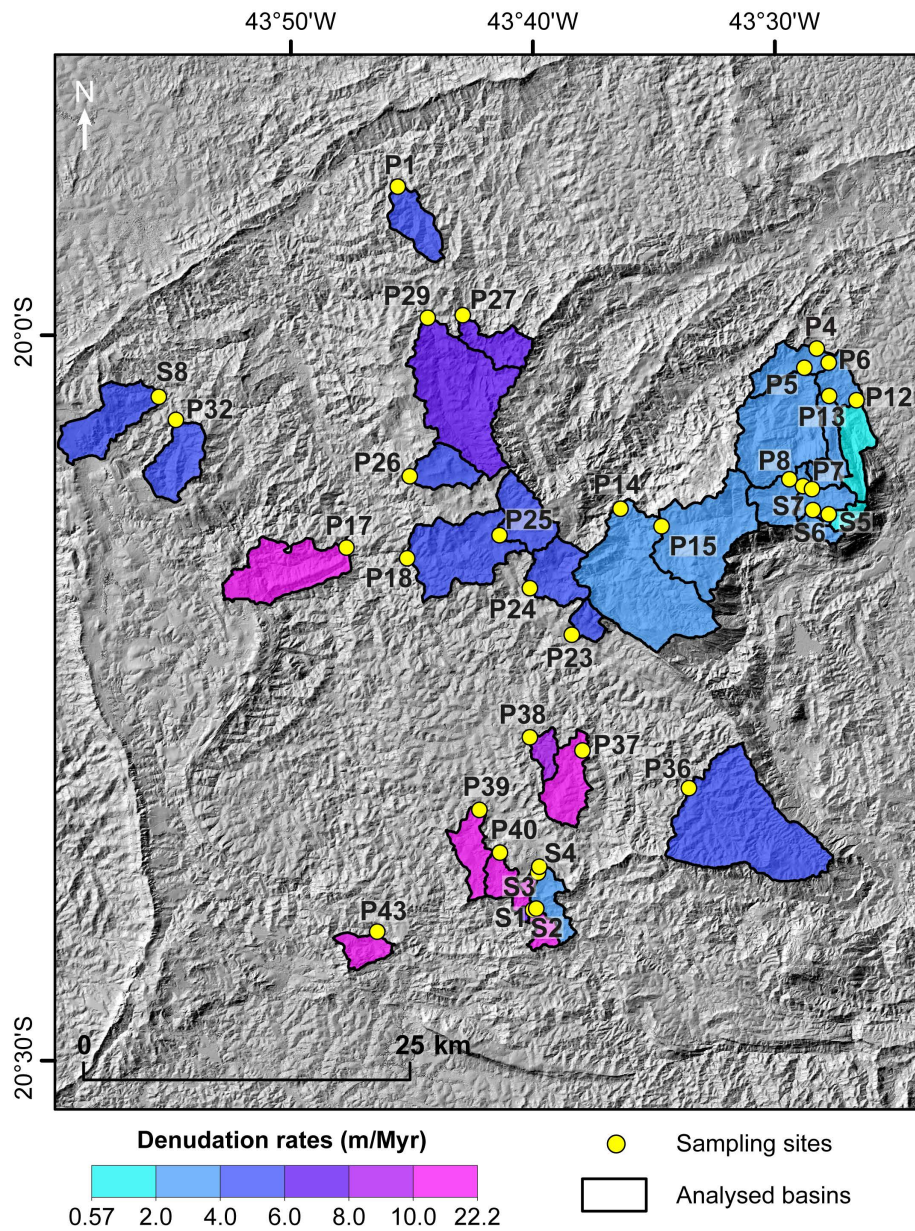


Figure 3: Catchment-averaged denudation rates in the study area draped over a hillshade image. Note that we identify as P'number' the 25 sampling sites of this study, whereas we label as S'number' the 8 sampling sites incorporated from Salgado et al. (2008). See Table S1 for ^{10}Be analytical results and derived denudation rate data.

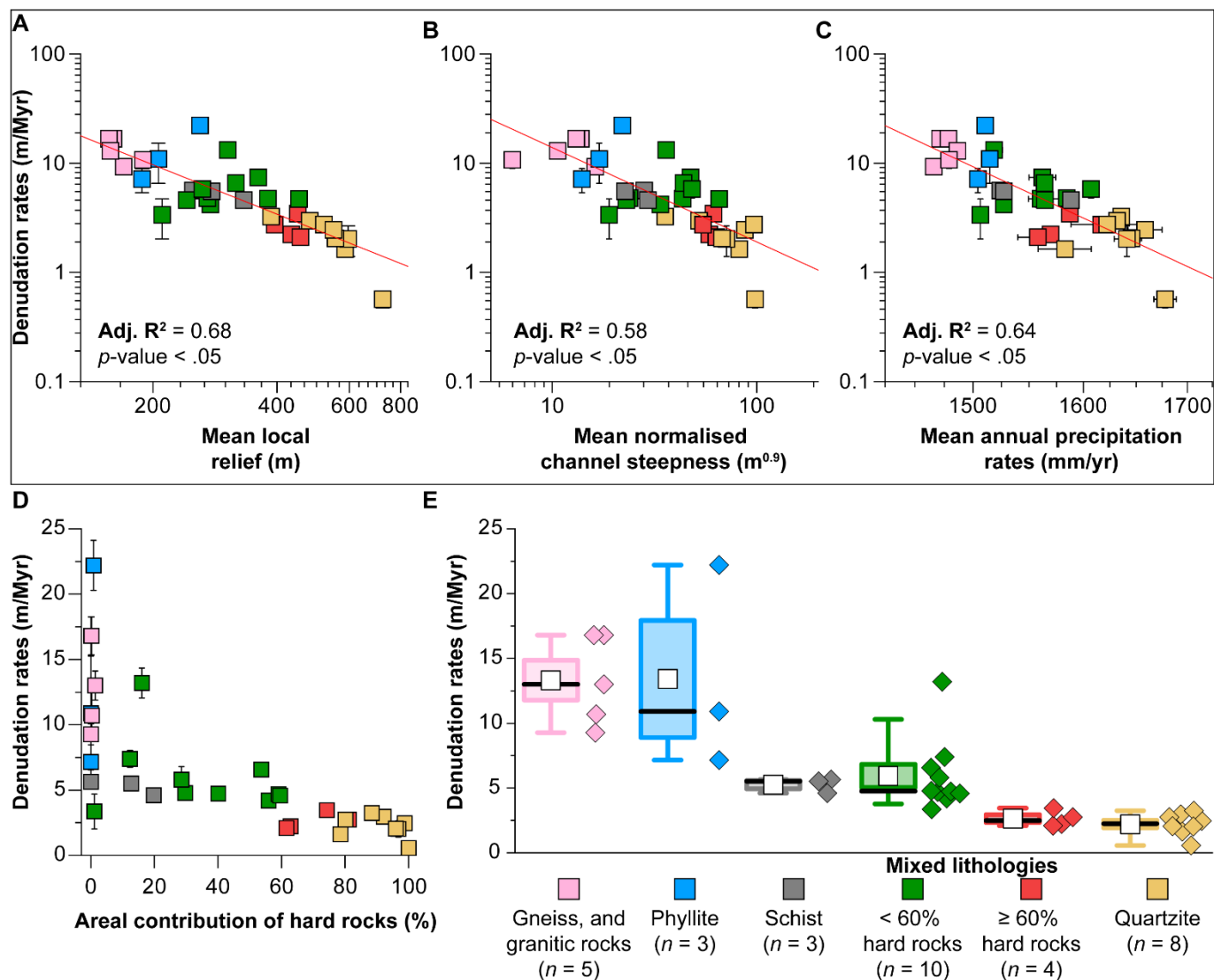
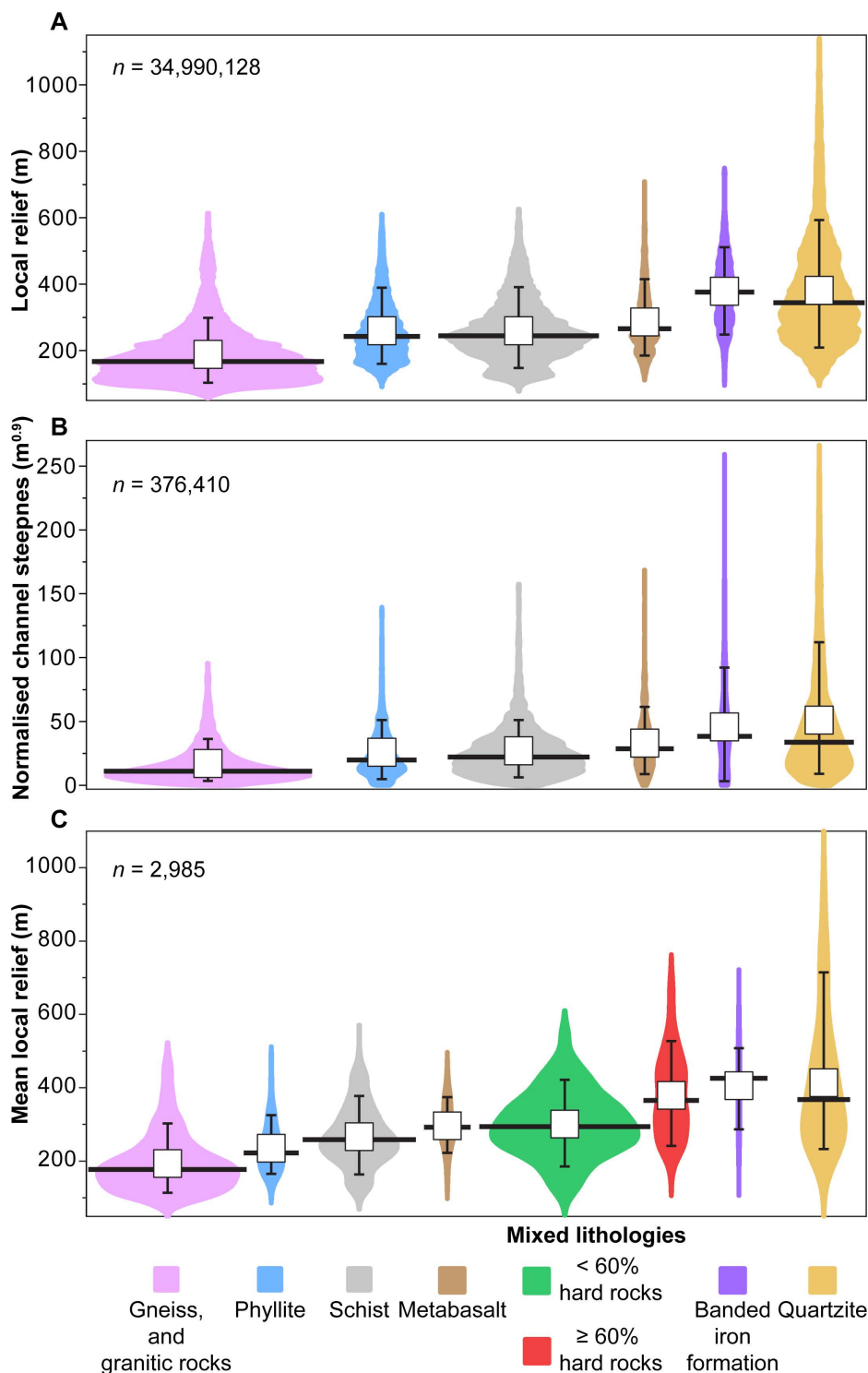
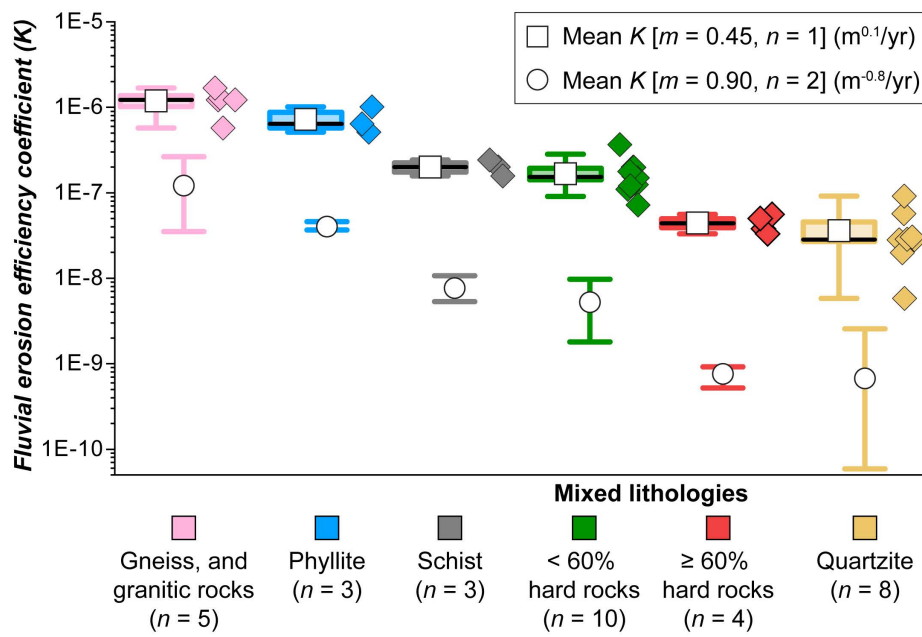


Figure 4: Links between denudation rates, geomorphic parameters, and rock type in the study area. Variations in catchment-averaged denudation rates with (A) mean local relief, (B) mean normalised channel steepness, (C) mean annual precipitation rates, and (D) percentage areal contribution of resistant rocks. Y-error bars show measurement errors in the nuclide concentration as well as errors related to the scaling method, and X-error bars indicate the SE of the mean. (E) Variations in catchment-averaged denudation rates per rock type, with the box on the left and raw data (diamonds) on the right. Box range represents the SE of the mean, whiskers show the interval between the 10th and 90th percentiles of the data, white squares show mean values, and thick black lines exhibit median values. Mixed lithology refers to catchments where a single lithology does not account for $\geq 75\%$ of the catchment area.



670 **Figure 5: Rock type controls topographic forms in the study area.** Violin plots show the probability density (smoothed by a kernel density estimator) of (A) local relief, (B) normalised channel steepness, and (C) catchment-averaged local relief, per rock type. Panels (A) and (B) represent the distribution of local relief and normalised channel steepness for the entire study area, whereas panel (C) shows mean values of local relief for all catchments with stream-order equal or higher than second-order (Strahler, 1957) underlain by the rock types represented in panels (A)–(C). Whiskers show the interval between the 10th and 90th percentiles of the data, white squares represent mean values, and thick black lines exhibit median values.



675 **Figure 6: Rock type controls variations in the fluvial erosion efficiency coefficient (K) in the study area.** Boxplot elements: box range
 represents the SE of the mean, whisker range shows the interval between the 10th and 90th percentiles of the data, and thick black line
 exhibit median values. Note that we calculated K assuming: ~~the slope exponent $n = 1$ and $n = 2$~~ i) $m = 0.45$ and $n = 1$ (derived values of K
 have units of $m^{0.1}/\text{yr}$), and ii) $m = 0.9$ and $n = 2$ (derived values of K have units of $m^{0.8}/\text{yr}$). For the case of $n = 1$, we show the boxplot on
 680 the left and raw data (diamonds) on the right. See Table S1 for data on each of the catchments analysed, including lithology and mean annual
 precipitation rates.

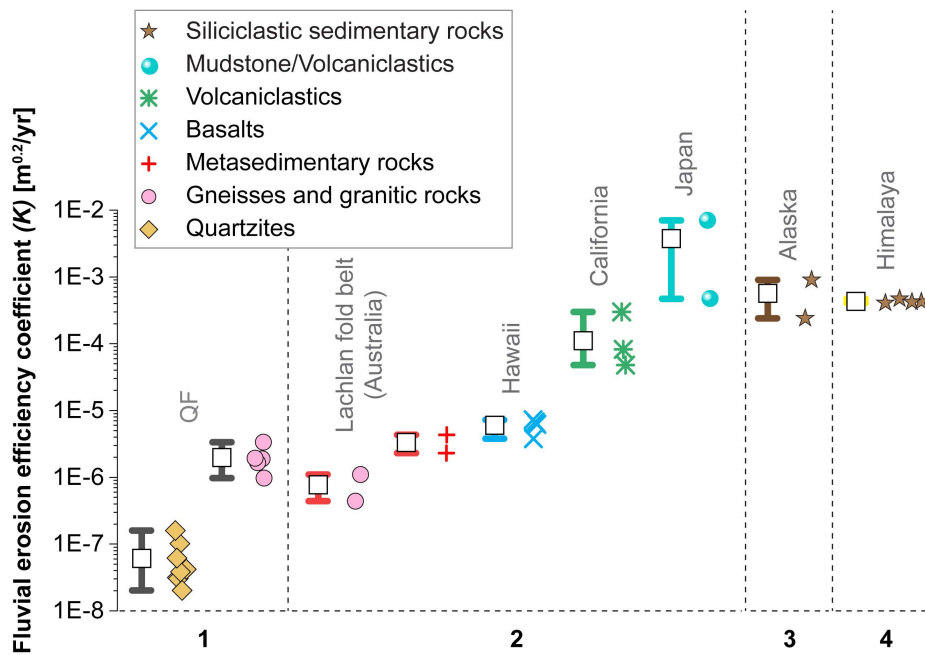


Figure 7: Comparison of our results for the fluvial erosion efficiency coefficient (K) with previously published estimates of K . Note that we display whiskers (representing the interval between the 10th and 90th percentiles of the data) and mean values (white squares) on the left and raw data (diamonds) on the right. Estimates of K were derived assuming the slope exponent $n = 1$. Numbers in the X-axis represent different data sources: (1) this study; (2) Stock and Montgomery (1999); (3) Whipple et al., (2000b); (4) Kirby and Whipple (2001). Lithology was compiled as described by authors.